THE ANNUAL REPORT OF THE MSU GROUP

(Jan.-Dec. 2000)

Contributors: V.B.Braginsky (P.I.), I.A.Bilenko, M.L.Gorodetsky,
F.Ya.Khalili, V.P.Mitrofanov, K.V.Tokmakov, S.P.Vyatchanin

Contents

I. SUMMARY

A. The reduction of the test mass oscillation damping caused by electrostatic actuator.

During the year 2000 V.Mitrofanov, K.Tokmakov and graduate student N.Styazhkina completed the study of the test mass oscillation damping produced by electrostatic actuators. The MSU group believes that usage of actuator directly applied to the mirror is inevitable. Thus the damping effect and correspondingly the fluctuating force acting on the mirror may be a serious obstacle to reach the planned sensitivity of the antenna. In the years 1998 and 1999 of the current grant the damping effect was observed and measured. The measurements have shown that this effect is a big one (see the MSU group reports of the years 1998 and 1999) and that it will substantially reduce the sensitivity. In the year 2000 different sources of damping were carefully analyzed and measured. Several sources were substantially reduced by appropriate choice of the actuators parameters. After this reduction it turned out that the key source of damping is associated with the property of the modelg of fused silica mirror. Special procedure of the flame treatment of this surface was proposed and tested. This treatment allowed to reduce the damping effect of the pendulum mode to the level smaller that $3 \times 10^{-9}\tilde{\text{w}}$hen the electrostatic actuator provided the dc force 10^{-4} N. This value of damping effect is smaller than the lowest damping measured till now in the test mass suspension. (See details in Appendix A).

B. The development and realization of methods of the excess noise measurement in the all fused silica fiber

The MSU group considers the problem of the excess noise in the high quality factor violin and pendulum modes in all fused silica suspension as one of the most important factors. In other words the unknown value of this noise may define the "fee" which has to be paid as some decrease of the sensitivity of the antenna and which cannot be precalculated.

In 1998 and 1999 dr. Bilenko and his students have proposed and tested two designs of the excess noise meter based on optical microspheres which promised to meet two important conditions: no any contaminations on the fiber's surface and high finesse in the optical readout systems (see previous annual reports). Both design failed to satisfy the second condition. In the year 2000 it was decided to get rid of microspheres and use a Fabry-Perot resonator (optical meter) with a small flat mirror ($4 \times 2 \times 1\,\mathrm{mm}^3$) made of pure fused silica welded in the middle of the tested fiber. The surface of this mirror had multilayer coating with high reflectivity. Two short fused silica sticks were welded to the opposite "corners" of the mirror before coating. The "free" ends of these sticks will be used for welding the fused silica fibers which noise will be measured. This design already was tested and the finesse higher than 40 was obtained, which allow to reach sensitivity at the level $3 \times 10^{-13} cm/\sqrt{Hz}$. This design guarantees that the coating will not be damaged by the welding of fibers. The assembling of all installation is in progress now, and the measurements of the violin mode noise will start in the close future.

C. The analysis of the thermo-refractive noise in the gravitational wave antenna

In the year 1999 the MSU group has reported the results of the analysis of two new sources of noise which may seriously change the antenna's sensitivity. In essence these sources are of nonlinear origin: namely due to nonzero value of the thermal expansion coefficient $\alpha_T = (1/l)\, dl/dT$ and due to the fluctuations of the temperature (thermodynamical temperature fluctuations in equilibrium and photo-thermal shot noise). The analysis has shown that these two sources of noise may decrease substantially the antenna's sensitivity (*Physics Letters A*, **A264** (1999) 1).

In the year 2000 the analysis of another source of noise was carried out by M. Gorodetsky and S. Vyatchanin (*Physics Letters A*, **A 271** (2000) 303). It is similar by origin by previous ones: the same fluctuations of temperature combined with nonzero value of the temperature dependence $\beta_T = (1/n)\, dn/dT$ of the refraction index n in the mirror's coating are producing

effective fluctuating change of the distance between the mirrors because a fraction of e.m. field is inside the mirror's coating. For usually used TiO_2 or Ta_2O_5 in the multilayer coating the value of β_T is larger than α_T for SiO_2, and the value of noise produced by thermo-refractive effect may "give contribution" to the total noise budget comparable with SQL (see Appendix C).

D. On the possibility to subtract the Brownian fluctuation in the mirror

It was shown by S. P. Vyatchanin and undergraduate student S. E. Strigin (*Physics Letters A*, **A272** (2000) 143) that the same thermo-refractive noise does not permit to measure the Brownian fluctuations in the mirror itself with sufficient accuracy in order to use this value for subtraction of this noise from the movement of the mirror's centers of mass (see part II of Appendix D).

E. The scheme of measurement of thermo-refractive noise

M. Gorodetsky has proposed and analyzed a simple scheme of experiment which allows to measure the thermo-refractive noise in fused silica. The basic idea is to use as a test object whispering gallery mode in fused silica microsphere. In this type of optical resonator (with the diameter $D \simeq 10^{-2}$ cm) the main part of e.m. field is inside the fused silica (in contrast with Fabri-Perot resonator). If the frequency of pumping wave is tuned to the slope of the resonance curve (the quality factor of the mode may exceed 10^9), the the thermo-refractive noise will be converted into random modulations of the output optic power. If the optimal mode of the resonator is used then the spectral density of the modulation of frequency will be at the level:

$$\sqrt{S_{\delta\omega/\omega}(\Omega)} \simeq 4 \times 10^{-12} \left(\frac{100\mu m}{D}\right)^{3/4} \left(\frac{1000 s^{-1}}{\Omega}\right)^{1/4} \frac{1}{\sqrt{Hz}}, \qquad (1)$$

where Ω is the frequency of analysis of fluctuations. This value may be observed if technical problems of modes' identification are solved (see details in Appendix E).

F. The analysis of the frequency fluctuations of nonlinear origin in self-sustained optical oscillators

To the best knowledge of MSU group members the theoretical analysis of the role of nonlinear origin noises in the pumping oscillator was not carried out till now. This analysis was done by S. P. Vyatchanin in the frame of this grant (*Physics Letters A*, accepted for publication). In the analysis the nonzero values of α_T and β_T were taken into account as well as back action noise. The net result of this analysis is that the thermo-refractive noise in NdYAG laser will dominate and that with 10 meter long reference cavity the pumping laser may have the frequency fluctuations at the level $10^{-20}\ 1/\sqrt{\mathrm{Hz}}$. This numerical estimate (based on certain parameters of the laser and the reference cavity) shows that the revision of the frequency noise of the pumping laser should be done as well as the condition for the level of symmetry in the two arms of the antenna (see Appendix F).

G. The analysis of the sensitivity of the discrete sampling variation measurement

According to the plan of researches the MSU group continued the analysis of different schemes and methods of measurement which may allow to circumvent the SQL value of the antenna sensitivity. In the year 2000 S.Danilishin, F.Khalili and S.Vyatchanin have completed the analysis of a new scheme of quantum meter. The first key task in this analysis was to eliminate the most inconvenient feature of the variation quantum measurement: the necessity to know apriori the arrival time and the shape of the signal because the hardware setup of the antenna depends on both of them.

This problem is solved. The basic feature of the new scheme of variation measurement is the discrete sampling: the procedure of the measurement is divided into many short intervals (shorter than the characteristic period of the signal). Thus the only necessary a priory knowledge is the upper frequency of the signal. The "fee" which has to be paid for this improvement is the rise of the amount of the energy pumped into the meter. It has to

be $720/\pi^4 \approx 7.4$ times bigger than in traditional quantum variation meter (see details in Appendix G).

II. APPENDIXES

Appendix A. Damping of the test mass oscillations caused by multistrip electrostatic actuator

Introduction

Laser interferometric gravitational wave detectors are now under construction by several groups around the world. The detectors test masses are the fused silica mirrors suspended by thin fibers to isolate them from perturbative forces. The mirrors' position and orientation are controlled by the low-noise servosystems to maintain the interferometer at the proper operating point. Magnetic actuators applied to produce the control forces can create relatively high excess noise [1]. As an alternative to the magnetic actuators, electrostatic systems using electrical forces were developed [2,3]. The multistrip electrostatic actuator that does not use a conductive coating on the mirror is the most promising one. It consists of series of plain strip electrodes alternatively at positive and negative potentials which are placed near the mirror surface.

The detailed analysis of forces produced by the multistrip electrostatic actuator was given in [4]. Another very important feature of the actuator is damping of the test mass oscillations caused by this actuator because in accordance with the fluctuation-dissipation theorem the excess damping of the test mass within the gravitational wave detector operating range of frequencies is a source of additional thermal noise. The articles devoted to the study of damping in torsion pendulums being under the action of the electrostatic force applied between an electrode placed on the pendulum bob and a nearby electrode were published recently [5–7]. This damping was found to depend on properties of the electrodes surfaces. In this article we present an analysis and measurements of the excess damping in the bifilar all-fused silica torsion pendulum which results from the electric field produced by the multistrip electrostatic actuator.

Experimental set-up

The experimental arrangement is shown in Fig.1. The torsion pendulum is a 0.5 kg fused silica cylinder, 7 cm in length and 6.5 cm in diameter suspended by two fused silica fibers 25 cm in length and $200\mu m$ in diameter. We used the cylinder with two fused silica cones that were hydroxide-catalysis bonded to the surface of the optical flat polished along the length of the cylinder. The fused silica cylinder with the bonded cones was manufactured and provided to us by S.Rowan and J.Hough from the University of Glasgow [8]. The pendulum damping associated with hydroxide-catalysis bonding was found not to exceed 4×10^{-9} [9]. The fused silica suspension fibers were welded to the cones. Top ends of the suspension fibers were welded to a fused silica disk that was attached through an indium gasket to the cover of the vacuum chamber rigidly fastened to a concrete wall. The chamber was evacuated to a pressure of about 10^{-7} Torr to minimize any damping of the pendulum modes due to the presence of residual gas.

The torsion mode of the pendulum was used to measure damping caused by the electric field of the electrostatic actuator. This mode has the Q-factor of about 10^8 due to the pendulum damping dilution factor [10]. Unlike the swing pendulum mode, there is no need to have a too large gap between the face of the cylinder and the actuator plate when using this mode. The amplitude of the swing motion for our pendulum must exceed approximately 5 mm in order to exclude the seismic perturbation effect on the Q measurement because the free decay change of the amplitude must be significantly greater than the change induced by seismic excitation of the pendulum.

The electrostatic actuator plate was mounted parallel to the end face of the suspended cylinder with a separating gap of $\approx 2 - 3$ mm. It was the fused silica plate, 5 cm in length, 3 cm in width and 1 cm in thickness. Two sets of gold strips were sputter-deposited on the polished surface of this plate. Each strip had the width of 4 mm and was separated from the next one by the 3 mm gap. One set of the strips was grounded. The voltage was applied to the other set of the strips. The center of the actuator plate was displaced from the center

of the cylinder by 1.5 cm to excite the torsion motion of the pendulum.

The amplitude of the torsion oscillation of the bifilar pendulum was monitored by the optical sensor that converted amplitude into the time interval measured by a counter. The laser beam to be reflected from the end face of the suspended cylinder was directed to the pair of 1 mm slits, with photodiodes placed behind them. Torsion oscillations of the pendulum resulted in a sequential pass of the light beam through the slits. The pulse signal was generated, whose duration determined the pendulum amplitude. The Q-factor was calculated from the measured decay time of free oscillations.

The electrostatic actuator was also used to excite the torsion oscillation of the pendulum. The ac exciting voltage at the frequency of the torsion mode (approximately 1.14 Hz) was added to the dc bias and was applied to electrodes of the actuator. When the amplitude of the torsion motion was excited to the appropriate level of ~ 0.05 rad the exciting voltage was switched off and the oscillation of the pendulum were allowed to decay freely.

Electrodes of the actuator were used also to monitor electrostatic charges sitting on the end face of the fused silica cylinder. In this case the electrodes were connected to the high impedance operation amplifier AD 549. The motion of the charged cylinder induced the charge on the actuator electrodes which resulted in the change of the amplifier input voltage. This system did not allow us to find the true magnitude and the charge distribution on the suspended fused silica cylinder end face. We could monitor however the charge total magnitude relative change and estimate roughly this magnitude. It was possible to change the electrostatic charge on the pendulum by switching on the ion pump for some chosen time interval (we used only turbomolecular pump to evacuate the chamber). Electrostatic charging of the fused silica pendulum due to ultraviolet radiation produced by an ion pump was searched in [11]. The electrostatic charge monitoring and its reduction by the means of the ion pump allowed us to be sure that the electric charge on the end face of the fused silica cylinder did not influence the measured damping.

Results of the measurements

In order to calibrate the actuator the ac voltage at the resonance frequency of the torsion mode was applied to the electrodes. The alternating torque produced by the actuator resulted in the change of the pendulum torsion amplitude which was measured. Basing on these results, we calculated the relation between the permanent torque M_e and the dc voltage U applied to the actuator as: $M_e = aU^2$ where a was found to be $\approx 4 \times 10^{-12} Nm/V^2$.

The torque M_e depends on the value of the gap between the actuator plate and the end face of the cylinder. Consequently, the actuator introduces the (negative) torsion stiffness $K_e \approx dM_e/d\theta$ (where θ is the angle of the torsion motion) in addition to the own pendulum torsion stiffness K . The ratio K_e/K can be found from the equation $K_e/K \approx 2\delta\omega/\omega$ valid when $|\delta\omega| \ll \omega$ where ω is the natural frequency of the pendulum torsion mode and $\delta\omega$ is the change in this frequency caused by the actuator. Fig. 2 shows the relative variation of the pendulum natural frequency as a function of the square of the dc voltage applied to the actuator.

The energy loss in the pendulum caused by the electric field of the actuator can be described through considering K_e as a complex number $K_e(1 - i\phi)$. An imaginary part ϕ is the parameter suitable to quantify the level of dissipation in the actuator. Then, the damping Q_e^{-1} of the pendulum associated with the electric field of the actuator can be expressed as $Q_e^{-1} \approx |K_e|\phi/K$ for $|K_e| \ll K$ and $\phi \ll 1$. This expression allows to separate out the dependence of Q_e^{-1} on the pendulum and the actuator parameters.

The damping Q_e^{-1} was determined in the experiments as a difference between reciprocals of the pendulum torsion mode Q-factors measured with and without the dc voltage applied to the actuator. The quality factor Q_0 of the pendulum in the absence of the electric field produced by the actuator was found to be $(7.5 \pm 0.7) \times 10^7$.

The experiments have shown that the damping Q_e^{-1} of the pendulum associated with the electric field of the multistrip electrostatic actuator strongly depended on properties of the suspended fused silica cylinder end surface. Fig. 3 shows the measured damping Q_e^{-1}

as a function of the dc voltage U applied to the actuator. Curve ($\Box$) was obtained for the mechanically polished end face of the fused silica cylinder cleaned in acetone and ethanol before evacuating the vacuum chamber with the pendulum in it. This curve is well fitted by U^2 dependence. Baking the chamber with the pendulum in it at the temperature of 110° C during 7 hours did not change the damping caused by the actuator.

Curve ($\diamond$) shows Q_e^{-1} measured after the thermal treatment of the fused silica cylinder end face by the flame of an oxygen/natural gas torch. This treatment was done by applying the flame directly to the surface of the cylinder and moving the flame back and forth across the surface. The duration of the flame treatment was about 10 minutes. Immediately afterwards the vacuum chamber with the pendulum in it was evacuated. The repeat flame treatment of the cylinder end face resulted in additional reduction of the damping Q_e^{-1} presented by curve ($\bullet$). After that the chamber was opened and the end face of the cylinder was covered with a sheet of paper wetted by water. After five hours the chamber was evacuated again. Accomplishing this procedure we did not observed a change in the damping within the limits of experimental error.

The flame treatment of the fused silica cylinder end face has changed some special feature of the pendulum damping caused by the electric field of the actuator. At low voltages the excess damping was not observed at the level within the resolution of the measurement, i.e. $Q_e^{-1} \approx 3 \times 10^{-9}$. This range of voltages became larger and ranged up to ≈ 760 V after the repeat procedure of the flame treatment. At this voltage applied to electrodes the actuator produced the torque of about 2.3×10^{-6} Nm acting on the fused silica cylinder. For the average moment arm of about 1.5×10^{-2} m this torque corresponded to the force in the order of 10^{-4} N. At the higher voltages the measured damping Q_e^{-1} weakly depended on voltage.

It was found that the damping Q_e^{-1} did not change depending on polarity of the applied voltage. The other important feature of the pendulum damping caused by the electric field of the electrostatic actuator is that it decreases if the ac electric voltage is applied instead of the dc voltage. In the case of the ac voltage with the frequency of 100 Hz and higher the

excess damping did not exceed 3×10^{-9} over all range of U used in our experiment.

Discussion

The damping of the pendulum caused by the electrostatic actuator is evidently associated with the electric field that varies as the pendulum oscillates. In general case damping of a mechanical oscillator due to an electric field may be caused by the number of different mechanisms, for example, the damping associated with eddy currents in the electrodes, the damping from the electric-field-induced coupling between the pendulum and the electrode, as well as the damping due to Joule loss in the electric circuit of the voltage source. The pendulum losses in our set-up caused by these mechanisms were small enough to be neglected. The most important loss mechanisms could be associated with the surface of the dielectric cylinder as well as with the surfaces of the metal electrodes.

The damping associated with metal electrodes may be caused by electron transitions between local surface states in the oxide and adsorbed layers or polarization of these layers under the action of the electric field. Gold coated electrodes were found to provide minimal losses [6,7,12]. Basing on these works, we may conclude that the losses associated with the gold electrodes of the actuator in our experiments has given a small contribution to the observed damping caused by the actuator.

The observed damping is evidently associated with electric losses on the surface of the suspended fused silica cylinder. Mechanical polishing of a fused silica sample results in the formation of the surface layer consisting of products of hydrolysis of SiO_2 and having the porous structure that can adsorb water [13]. The flame treatment is likely to remove this layer.

It is interesting to compare our results with those presented in [14]. The authors have found flame polishing had reduced surface mechanical losses in a fused silica sample and had allowed them to reach the lowest measured at the room temperature value of the intrinsic mechanical loss in fused silica. The procedure of flame polishing was nearly identical to

the flame treatment described in this article. The warming-up was not so deep in our case. Nevertheless the flame treatment reduced surface electric losses in the fused silica cylinder.

The results reported here show that the damping of fused silica test mass oscillation caused by the multistrip electrostatic actuator producing forces of the order of 10^{-4} N can be reduced to the level of less than 3×10^{-9}. This value is lower than the lowest damping measured up to now in the pendulum mode of a prototype fused silica test mass suspension for use in interferometric gravitational wave detectors.

FIGURES

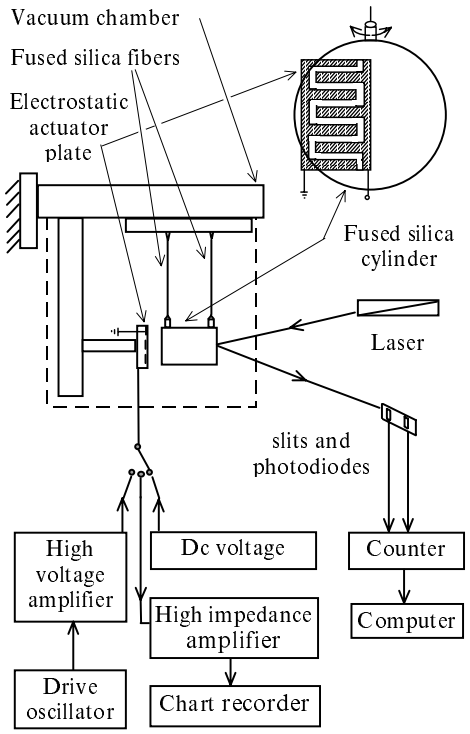

FIG. 1. Experimental arrangement used to measure damping caused by the electrostatic actuator.

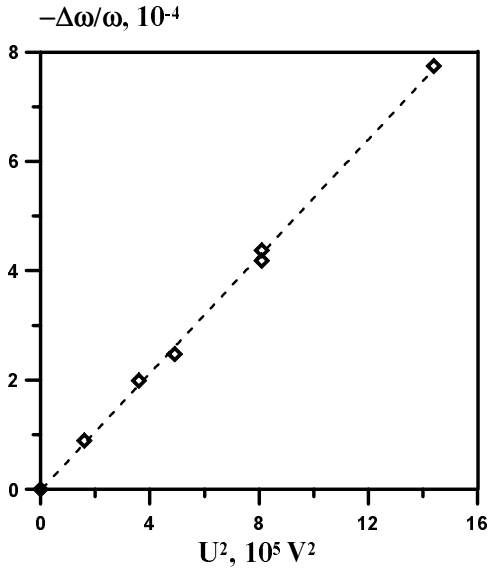

FIG. 2. Relative variation of the pendulum natural frequency $-\delta\omega/\omega$ as a function of the square of dc voltage U^2 applied to the actuator.

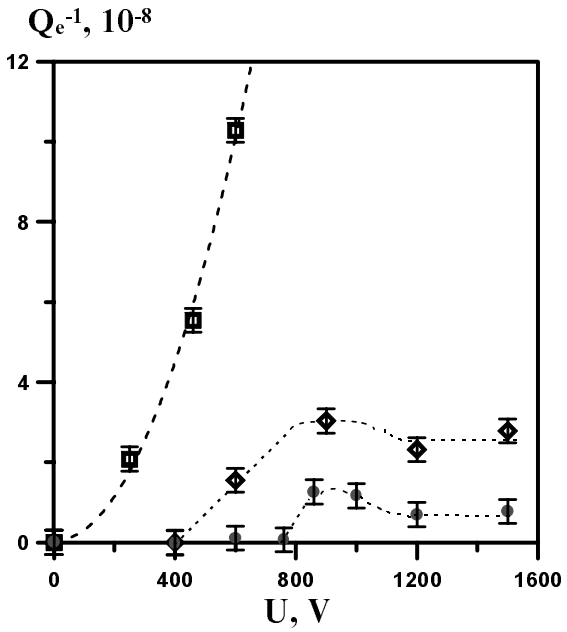

Figure 3. Variation of the pendulum damping Q_e^{-1} as a function of dc voltage U applied to the actuator.

(□) – before the flame treatment;

(◊) – after the first flame treatment;

(•) – after the repeat flame treatment.

REFERENCES

[1] A. Abramovici, W. Althouse, J. Camp, D. Durance, J. A. Giame, A. Gillespie, S. Kawamura, A. Kuhnert, T. Lyons, F. J. Raab, R. L. Savage, D. Shoemaker, L. Sievers, R. Spero, R.Vogt, R. Weiss, S. Whitcomb and M. Zucker, Phys. Lett. A 218 (1996) 157.

[2] P. S. Linsay and D. H. Shoemaker, Rev. Sci. Instrum. 53 (1982)1014.

[3] A. Cadez and A.Abramovici, J.Phys. E 21 (1988) 453.

[4] S. Grasso, C. Altucci, F. Barone, V. Ragozzino, S. Solimeno, Pham-Tu, J. – Y. Vinet, R. Abbate, Phys.Let.A 244 (1998) 360.

[5] V. P. Mitrofanov, N. A. Styazhkina, Phys.Lett.A 256 (1999) 351.

[6] C. C. Speake, R. S. Davis, T. J. Quinn and S. J. Richman, Phys. Lett. A 263 (1999) 219.

[7] E. Willemenot and P. Touboul, Rev.Sci.Instrum. 71 (2000) 302.

[8] S. Rowan, S. M. Twyford, J. Hough, D.-H. Gwo and R. Route, Phys. Lett. A 246 (1998) 471.

[9] K. Tokmakov, V. Mitrofanov, V. Braginsky, S. Rowan and J. Hough, in Gravitational Waves, proceedings of the Third Edoardo Amaldi Conference ed. S. Meshkov, Melville NY: American Institute of Physics, 2000, p.445.

[10] V. B. Braginsky, V. P. Mitrofanov, K. V. Tokmakov, Phys.Lett.A 218 (1996) 164.

[11] S. Rowan, S. Twyford, R. Hutchins and J. Hough, Class.Quantum.Grav. 14 (1997) 1537.

[12] V. P. Mitrofanov and N. A. Styazhkina, Rev.Sci.Instrum. 71 (2000) 3905.

[13] B. S. Lunin, S. N. Torbin, M. N. Danchevskaya and I. V. Batov, Moscow Univ. Chemistry Bulletin 35 (1994) 24, Allerton Press, Inc.

[14] S. D. Penn, G. M. Harry, A. M. Gretarsson, S. E. Kittelberger, P. R. Saulson, J.

J. Schiller, J. R. Smith and S. O. Swords, Syracuse University Gravitational Physics Preprint 2000/8-11.

Appendix C. Thermo-refractive noise in gravitational wave antennae

Introduction

We have shown in our previous article [4] that thermodynamical fluctuations of temperature in mirrors (test masses) of LIGO-type gravitational wave antenna [1,2] are transformed due to the thermal expansion coefficient $\alpha = (1/l)(dl/dT)$ into additional (thermoelastic) noise which may be a serious "barrier" limiting sensitivity. This noise is caused in fact by random fluctuations of the coordinate averaged over the mirror's surface. The spectral density of this random coordinate displacement may be presented for infinite test mass in the following form [1]:

$$S^{\rm TE}_{x,\,\alpha}(\omega) = \frac{8}{\sqrt{2\pi}}\,\frac{\kappa T^2\alpha^2(1+\sigma)^2\,\lambda^*}{(\rho C)^2\,r_0^3\,\omega^2}. \qquad (2)$$

Here κ is the Boltzmann constant, T is temperature, σ is Poison ratio, λ^* is thermal conductivity, ρ is density and C is specific heat capacity, r_0 is the radius of the spot of laser beam over which the averaging of the fluctuations is performed. This noise is of nonlinear origin as the nonzero value of α is due to the anharmonisity of the lattice.

The goal of this article is to present the results of the analysis of another additional (and also of nonlinear origin) effect which may be comparable with other known noise mechanisms limiting the sensitivity. Qualitatively this effect is may be understood in the following way. The laser beam "extracts" the information not only about the change of the length of the antenna produced by gravitational wave but also about the fluctuations of position of mirrors' surfaces averaged over the beam spot. These fluctuations lead to phase noise in the reflected optical field. However the phase noise may be produced by another effect. High reflectivity of the mirrors is provided by multilayer coatings which consist of alternating

---

[1] This result was refined for the case of finite test masses by Yu. T. Liu and K. S. Thorne [6]. However the difference from our calculation is only several percents for the planned sizes of test masses, and hence we use here much more compact expression (2).

sequences of quarter-wavelength dielectric layers having refraction indices n_1 and n_2. The most frequently used pairs of layers are $TiO_2 - SiO_2$ and $Ta_2O_5 - SiO_2$. While reflecting * the optical wave "penetrates" in the coating on certain depth. This depth is of the order of the optical thickness of one pair of layers $l < 1\mu$. If the values of n_1 and n_2 depend on temperature T (thermo-refractive factor $\beta = dn/dT$ is nonzero) then thermodynamical fluctuations of temperature lead to fluctuations of optical thickness of these layers and hence to the phase noise in the reflected wave. Though the thickness l of the working layer is small, the coefficient β is usually significantly larger than α (both have the same dimensions). For fused silica (SiO_2) $\alpha = 5 \times 10^{-7}\ K^{-1}$ and $\beta = 1.45 \times 10^{-5}\ K^{-1}$ (i.e. 30 times larger than α). This phase noise may be evidently easily recalculated in terms of equivalent fluctuations of the surface and consequently compared with the spectral sensitivity of the antenna.

We have analyzed also the photo-thermal refractive shot noise: due to random absorption of optical photons, the random fluctuations of temperature in the surface layer of the mirror take place, producing fluctuations of refractive indices of the coating and therefore phase fluctuations of reflected light wave (this effect is similar to photo-thermal shot noise, analyzed in [4]). However, this effect is numerically much smaller than thermo-refractive noise — that is why we do not present here the detailed analysis of it.

Thermo-refractive noise

The theory of reflection of light from multilayer dielectrical coating is well known (see for example [5]). Using traditional approach we may recalculate the phase shift $\delta\phi$ into equivalent displacement δx of mirror (see Appendix C1):

$$\delta x = \frac{\lambda}{4\pi}\delta\phi = -\bar{u}\lambda\beta_{\text{eff}}, \tag{3}$$

$$\beta_{\text{eff}} = \frac{n_2^2\beta_1 + n_1^2\beta_2}{4(n_1^2 - n_2^2)}. \tag{4}$$

Here $\bar{u}$ is the fluctuation of averaged temperature, $\beta_1 = dn_1/dT$, $\beta_2 = dn_2/dT$. It is important to note, that effective coating thickness is much smaller than the characteristic

length of diffusive heat transfer: $l \ll a/\sqrt{\omega}$ (a is temperature conductivity, ω is the frequency of observation which is of order $\sim 100Hz$ for laser gravitational wave antenna). Therefore we may consider in our calculations that fluctuations of temperature are correlated in the layers.

To calculate thermodynamical fluctuations of temperature $u(\vec{r},t)$ in the surface layers we use Langevin approach and introduce fluctuational thermal sources $F(\vec{r},t)$ added to the right part of the equation of thermal conductivity:

$$\frac{\partial u}{\partial t} - a^2 \Delta u = F(\vec{r},t), \qquad a^2 = \frac{\lambda^*}{\rho C}. \tag{5}$$

This approach was described and verified in [4] (see all the details over there). As in [4] we replace the mirror by half-space: $-\infty < x < \infty,\ -\infty < y < \infty,\ 0 \le z < \infty$ with the boundary condition of thermo-isolation on surface $z = 0$. We may now calculate the spectrum of temperature fluctuations:

$$u(\vec{r},t) = \int_{-\infty}^{\infty} \frac{d\vec{k}\, d\omega}{(2\pi)^4}\, u(\omega,\vec{k}) e^{i\omega t + i\vec{k}\vec{r}}, \tag{6}$$

$$u(\omega,\vec{k}) = \frac{F(\vec{k},\omega)}{a^2(\vec{k})^2 + i\omega}, \tag{7}$$

$$\begin{aligned} \langle F(\vec{k},\omega) F^*(\vec{k}_1,\omega_1)\rangle &= \frac{2\kappa T^2 \lambda^*}{(\rho C)^2}\,(2\pi)^4 |\vec{k}|^2\, \delta(\omega-\omega_1)\times \\ &\times\, \delta(k_x - k_{x1})\,\delta(k_y - k_{y1})\times \\ &\times\, [\,\delta(k_z - k_{z1}) + \delta(k_z + k_{z1})\,]. \end{aligned} \tag{8}$$

The thermodynamical fluctuations of temperature $\bar{u}$ averaged over the volume $V = \pi r_0^2 l$ may be presented in the following form:

$$\begin{aligned} \bar{u} &= \frac{1}{\pi r_0^2 l} \int_{-\infty}^{\infty} dx dy \int_0^{\infty} dz\ u(\vec{r},t)\ e^{-(x^2+y^2)/r_0^2}\, e^{-z/l} = \\ &= \int_{-\infty}^{\infty} \frac{d\vec{k}\, d\omega}{(2\pi)^4}\, \frac{F(\vec{k},\omega) e^{i\omega t}}{a^2|\vec{k}|^2 + i\omega}\ e^{-(k_x^2+k_y^2)r_0^2/4} \frac{1}{1 - ik_z l}, \end{aligned} \tag{9}$$

From this expression and from (8) we find immediately the spectral density $S_u(\omega)$ of fluctuations of the averaged temperature:

$$S_u(\omega) = 2 \times \frac{2\kappa T^2\,\lambda^*}{(\rho C)^2} \int_0^\infty \frac{2\pi\, k_\perp dk_\perp}{(2\pi)^2} \int_{-\infty}^\infty \frac{dk_z}{2\pi} \times$$
$$\times \frac{k_z^2 + k_\perp^2}{a^4(k_z^2 + k_\perp^2)^2 + \omega^2}\; e^{-k_\perp^2 r_0^2/2} \frac{(1+1)}{1 + k_z^2 l^2} =$$
$$\simeq \frac{\sqrt{2}\,\kappa T^2}{\pi\, r_0^2 \sqrt{\omega \lambda^* \rho C}} \qquad (10)$$

Here $k_\perp^2 = k_x^2 + k_y^2$. The first term 2 appears because as in [4] we use "one-sided" spectral density, defined only for positive frequencies, which is connected with the correlation function $\langle u(t)u(t+\tau)\rangle$ by the formula $S_u(\omega) = 2\int_{-\infty}^{\infty} d\tau\, \langle u(t)u(t+\tau)\rangle\, \cos(\omega\tau)$. The term $(1+1)$ appears due to two δ-functions in square brackets in (8). For the frequency of observation $\omega \simeq 2\pi \times 100$ s^{-1} characteristic length $a/\sqrt{\omega} \simeq 50\ \mu$ (we used for the estimates constants for fused silica), so that $l \ll a/\sqrt{\omega} \ll r_0$. Taking into account that $k_\perp \simeq 1/r_0 \ll \sqrt{\omega}/a$ we may consider the first denominator as constant while integrating over $k_\perp$. In the same way $k_z \simeq 1/l \gg \sqrt{\omega}/a$ and while integrating over k_z we may consider the second denominator as unity. It is interesting that in this model the spectral density $S_u(\omega)$ does not depend on l.

This spectral density may be recalculated to the spectral density of equivalent fluctuations of surface displacement to compare it with other known sources of noise:

$$S^{TD}_{x,\,\beta}(\omega) = \frac{\sqrt{2}\,\beta_{eff}^2 \lambda^2 \kappa T^2}{\pi r_0^2 \sqrt{\omega \rho C \lambda^*}}, \qquad (11)$$

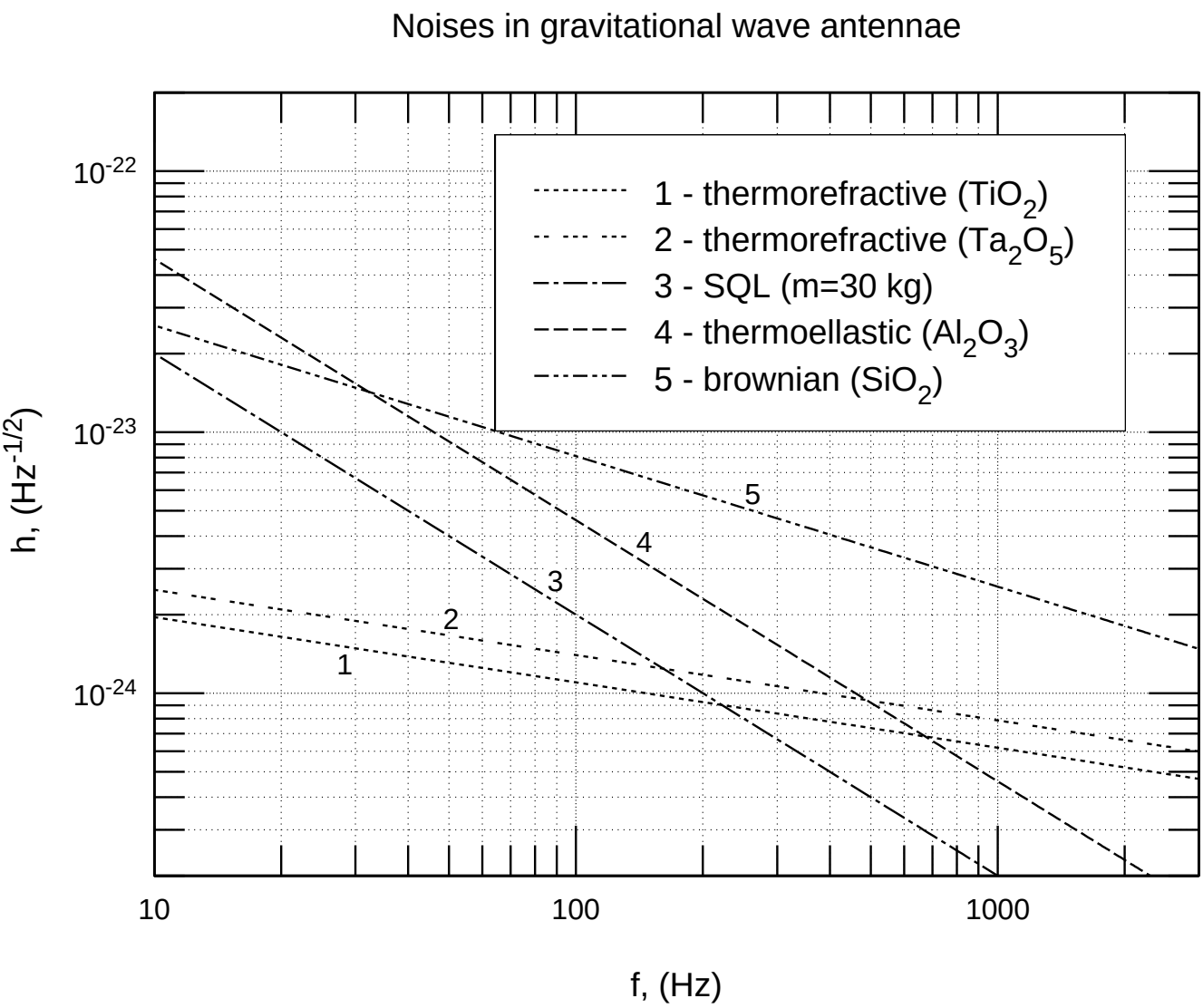

FIG. 3. Comparison of SQL-limited sensitivity with different sources of noise in gravitational wave antennae: thermo-refractive, Brownian (dominating in fused silica mirrors) and thermo-elastic (dominating in sapphire mirrors).

Numerical estimates

For the numerical estimates we assumed that the multilayer coating consists from alternating pairs of layers: TiO_2 ($n_1 = 2.2$) and SiO_2 ($n_2 = 1.45$), or Ta_2O_5 ($n_1 = 2.2$) and SiO_2 ($n_2 = 1.45$). The values of β for TiO_2 and for Ta_2O_5 were found in [9].

We want now to compare the thermo-refractive fluctuations with thermoelastic noise (2) and noise associated with the mirrors' material losses described in the model of structural

damping [10] (we denote it as Brownian motion of the surface). In this model the angle of losses ϕ does not depend on frequency and for its spectral density the following formula is valid for infinite test mass [8,4,6]:

$$S_x^{\rm B}(\omega) \simeq \frac{4\kappa T}{\omega} \frac{(1-\sigma^2)}{\sqrt{2\pi} E r_o} \phi, \tag{12}$$

where E is Young modulus, and σ is Poison ratio.

The spectrsal sensitivity of gravitational wave antenna to the perturbation of metric $h(\omega)$ may be recalculated from noise spectral density of displacement x using the following formula:

$$h(\omega) = \frac{\sqrt{2(S_{x,r_{01}}(\omega) + S_{x,r_{02}}(\omega))}}{L}, \tag{13}$$

where we used the fact that antenna has two arms (with length L) with two mirrors the fluctuations on which are averaged over the radii r_{01} and r_{02}.

The LIGO-II antenna will approach the level of SQL, so we also compare the noise limited sensitivity to this limit in spectral form [9]:

$$h_{\rm SQL}(\omega) = \sqrt{\frac{8\hbar}{m\omega^2 L^2}}. \tag{14}$$

For the calculations we used the set of parameters given in Appendix C2 (the same as in [4]) plus [9] *

$$\begin{aligned}
&r_{01} = 3.6/\sqrt{2}\ \text{cm}, \quad r_{02} = 4.6/\sqrt{2}\ \text{cm},\\
&n_1 = 2.2, \qquad \beta_2 = 4\cdot 10^{-5}\ \text{K}^{-1} \quad (TiO_2),\\
&n_1 = 2.2, \qquad \beta_2 = 6\cdot 10^{-5}\ \text{K}^{-1} \quad (Ta_2O_5),\\
&n_2 = 1.45, \qquad \beta_1 = 1.5\cdot 10^{-5}\ \text{K}^{-1} \quad (SiO_2),
\end{aligned}$$

We used figures from [9] for ion plating method only, for other methods of deposition the value of β may be two times larger. In figure 1 we plot all previously known noises [4] together with the new one. We see that thermorefractive noise limitation is close to SQL * for the frequences near 200 Hz.

Conclusion

Summing up, we may say that thermo-refractive effect is not small and it must be seriously considered in interferometric gravitational antennae (projects LIGO-II and especially LIGO-III, where overcomming of the SQL is planned). It is also important that this effect depends slower on the radii of the beam-spots than thermo-elastic noise and thus may become dominating for larger r_0 planned in LIGO-II and LIGO-III.

Appendix C1. Coefficient of reflection

In this appendix we give the calculation of coefficient of reflection of light wave from multilayer coatings consisting of infinite sequences of pairs of quarter-wavelength dielectrical layers n_1 and n_2.

Let the refraction index of odd layers fluctuates on Δn_1 and the refraction index of even layers on Δn_2. One may reformulate this problem into the problem for distributed long line [5]. The equivalent impedance Z of this system of layers may be deduced using the following statement: the addition of two layers does not change the value of Z.

Voltage V_2 and current I_2 at the end of second layer may be found from input voltage V_0 and current I_0 using transformation matrix M ([5], formula (3.9.27)):

$$\begin{pmatrix} V_2 \\ I_2 \end{pmatrix} = M \times \begin{pmatrix} V_0 \\ I_0 \end{pmatrix}, \quad M = \begin{pmatrix} M_{11} & M_{12} \\ M_{21} & M_{22} \end{pmatrix},$$

$$M_{11} = \cos\phi_1 \cos\phi_2 - \frac{n_1}{n_2} \sin\phi_1 \sin\phi_2,$$

$$M_{12} = -i \left(\frac{\sin\phi_1 \cos\phi_2}{n_1} + \frac{\sin\phi_2 \cos\phi_1}{n_2} \right),$$

$$M_{21} = -i \left(n_2 \sin\phi_2 \cos\phi_1 + n_1 \sin\phi_1 \cos\phi_2 \right),$$

$$M_{22} = \cos\phi_1 \cos\phi_2 - \frac{n_2}{n_1} \sin\phi_1 \sin\phi_2,$$

$$M \simeq \begin{pmatrix} -\frac{n_1}{n_2} & i\left(\frac{\varphi_2}{n_1} + \frac{\varphi_1}{n_2}\right) \\ i\left(n_2\varphi_1 + n_1\varphi_2\right) & -\frac{n_2}{n_1} \end{pmatrix}$$

Here we take into account that for quarter-wavelength layers $\phi_1 = \pi/2 + \varphi_1$, $\phi_2 = \pi/2 + \varphi_2$ and therefore one may use approximation $\sin\phi_1 \simeq 1$, $\sin\phi_2 \simeq 1$, $\cos\phi_1 \simeq -\varphi_1$, $\cos\phi_2 \simeq -\varphi_2$.

Now we put that $I_0 = YV_0$ and $I_2 = YV_2$ ($Y = 1/Z$ is generalized conductivity of the sequence of layers) and obtain two equations:

$$V_2 = V_0\left(-\frac{n_1}{n_2} + iY\left(\frac{\varphi_2}{n_1} + \frac{\varphi_1}{n_2}\right)\right), \tag{15}$$

$$YV_2 = V_0\left(i\left(n_2\varphi_1 + n_1\varphi_2\right) - Y\frac{n_2}{n_1}\right). \tag{16}$$

Solving these equations we find conductivity Y and reflection coefficient K:

$$Y \simeq -i\,\frac{n_1 n_2}{n_1^2 - n_2^2}\left(n_2\varphi_1 + n_1\varphi_2\right), \tag{17}$$

$$K = \frac{Y-1}{Y+1} \simeq -1 - 2i\,\frac{n_1 n_2}{n_1^2 - n_2^2}\left(n_2\varphi_1 + n_1\varphi_2\right) \tag{18}$$

From this point it is easy to obtain (3,4), assuming

$$\varphi_1 = \frac{\pi}{2}\frac{\Delta n_1}{n_1}, \qquad \varphi_2 = \frac{\pi}{2}\frac{\Delta n_2}{n_2}$$

Appendix C2. Parameters

$\omega = 2\pi \times 100\ \mathrm{s}^{-1}$, $T = 300$ K,

$m = = 3 \times 10^4$ g, $\lambda = 1.06\ \mu$, $L = 4 \times 10^5$ cm;;

Fused silica:

$\alpha = 5.5 \times 10^{-7}\ \mathrm{K}^{-1}$, $\lambda^* = 1.4 \times 10^5\ \dfrac{\mathrm{erg}}{\mathrm{cm\ s\ K}}$,

$\rho = 2.2\ \dfrac{\mathrm{g}}{\mathrm{cm}^3}$, $C = 6.7 \times 10^6\ \dfrac{\mathrm{erg}}{\mathrm{g\ K}}$,

$E = 7.2 \times 10^{11}\dfrac{\mathrm{erg}}{\mathrm{cm}^3}$, $\sigma = 0.17$, $\phi = 5 \times 10^{-8}$;

Sapphire:

$\alpha = 5.0 \times 10^{-6}\ \mathrm{K}^{-1}$, $\lambda^* = 4.0 \times 10^6\ \dfrac{\mathrm{erg}}{\mathrm{cm\ s\ K}}$,

$\rho = 4.0\ \dfrac{\mathrm{g}}{\mathrm{cm}^3}$, $C = 7.9 \times 10^6\ \dfrac{\mathrm{erg}}{\mathrm{g\ K}}$,

$E = 4 \times 10^{12}\,\dfrac{\mathrm{erg}}{\mathrm{cm}^3}$, $\sigma = 0.29$, $\phi = 3 \times 10^{-9}$.

REFERENCES

[1] V. B. Braginsky, M. L. Gorodetsky, and S. P. Vyatchanin, *Physics Letters* **A 264**, 1 (1999); cond-mat/9912139;

[2] A. Abramovici *et al.*, Science **256**(1992)325.

[3] A. Abramovici *et al.*, Phys.Letters.A **218**, 157 (1996).

[4] Yu. T. Liu and K. S. Thorne, submited to *Phys. Rev. D.*

[5] S. Solimeno, B. Crosignani and P. Diporto, *Guiding, Diffraction and Confinement of Optical Radiation*, Academic Press, 1986.

[6] P. R. Saulson, *Rhys. Rev. D*, **42**, 2437 (1990);
G. I. Gonzalez and P. R. Saulson, *J. Acoust. Soc. Am.*, **96**, 207 (1994).

[7] F. Bondu, P. Hello, Jean-Yves Vinet, *Physics Letters* **A 246**, 227 (1998).

[8] V. B. Braginsky, M. L. Gorodetsky, F. Ya. Khalili and K. S. Thorne, *Report at Third Amaldi Conference, Caltech*, July, 1999.

[9] *Thin films for optical systems* (for the International Journal of Optoelectronics), Ed: F Flory, Marcel Dekker Inc, ISBN 0 8247 96333 0, 1995.

Appendix D. The problem of compensation of internal mechanical noise in test mass of gravitational wave antennae

Introduction

Fluctuations of reflecting surface of test mass relatively its center of mass (the internal mechanical noise in test mass) is one of key problems in the full scale terrestrial interferometric gravitational wave antennae (projects LIGO-II, VIRGO, GEO-600, TAMA), which have to be solved in order to achieve in year 2005 the planned sensitivity in units of amplitude of the perturbation of metric at the level $h \simeq 2 \times 10^{-23}$ which corresponds to the Standard Quantum Limit (SQL). At this level the quantum features of macroscopic body behavior became essential. Fused silica used as a material for first stage of antenna (LIGO-I, VIRGO) [1,2] has a disadvantage — relatively large Brownian internal noise. We will call as Brownian the fluctuations which are usually calculated from phenomenological model of structural losses in the material in order to distinguish them from thermoelastic noise. There was some optimism after the proposals to use sintetic sapphire instead of fused silica because of Brownian noise in sapphire is much less. Unfortunately the thermoelastic noise happens to be too large in sapphire — it was demonstrated in [4] for model of infinite test mass. The physical origin of thermoelastic noise is fundamental thermodynamical fluctuations of temperature which causes variation of test mass shape due to thermal expansion. This result was refined by Yu. T. Liu and K. S. Thorne [6] for finite test mass (the difference between spectral densities of internal noise for infinite and finite size test mass does not increase several percents for planned sizes of test mass).

In this paper we discuss "the last line of defense" against internal noise — the possibility of compensation. It is not a new idea: in [5] there was demonstrated the possibility of compensation of suspension noise of test mass (the fluctuations of test mass position caused by thermal noise in suspension fiber) using additional measurement of horizontal displacement of fiber averaged by proper way over its length and subsequent subtraction from antenna

interferometer readout.

In order to realize compensation of internal mechanical noise we must have the possibility to measure *independently* the coordinate of test mass surface $Z_{\rm spot}$ averaged over laser beam crossection with radius r_0:

$$Z_{\rm spot} = \frac{1}{\pi r_0^2} \int_0^R r\, dr \int_0^{2\pi} d\phi\ e^{-r^2/r_0^2}\, v_z(r,\phi)|_{z=0}, \tag{19}$$

where $v_z(r,\phi)$ – is the fluctuational displacement of test mass surface in normal direction to surface at point with coordinates r and ϕ. Below we use cylindrical coordinate system which axis coincides with axis of cylindrical test mass having radius R and height H, face surface has coordinate $z = 0$ and back surface — $z = H$.

Let us imagine that we have ideal position meter which error of measurement is negligible small. Then the key problem for compensation is to define the support body, i.e. body relatively to which position we measure the coordinate $Z_{\rm spot}$. The best variant would be to measure relatively center of mass of our test mass. However center of mass is inaccessible for measurement. If we measure the spot coordinate relatively some support body we measure the difference $\delta Z = Z_{\rm spot} - Z_{\rm body}$ between coordinate of spot and coordinate $Z_{\rm body}$ of support body. Therefore additional noise caused by fluctuations of support body position is inevitably introduced. Indeed instead of measurement the value $Z_{\rm spot}$ one measures another value δZ and the accuracy of compensation will be defined by difference between these values, i.e. by $Z_{\rm body}$. So one can proclaim as Archimed that for absolute compensation the "point of support" is necessary even if the ideal meter is available.

In this paper we discuss one of the possibilities, which could be realized easier by experiment. It is measurement of the difference $\Delta Z = Z_{\rm spot} - Z_{\rm back}$ between spot coordinate $Z_{\rm spot}$ and coordinate

$$Z_{\rm back} = \frac{1}{\pi R^2} \int_0^R r\, dr \int_0^{2\pi} d\phi\ v_z(r,\phi)|_{z=H},$$

averaged over back surface of test mass. It is known that the larger the square of averaging the smaller the fluctuations of averaged coordinate. That is why we consider coordinate $Z_{\rm back}$ averaged all over the back wall of the test mass.

In section II we discuss how much can be the value of compensation if ideal position meter is used for measurement ΔZ. We show that using compensation one can overcome SQL several times. However it is worth underlining that result numbers given in table I express the point of view of *extreme* optimism, who assumes that experimentalist can create ideal meter with *any* required properties. Unfortunately the reality is considerably more tough.

Being optimists in section II we try to become realists in section II where we consider the variant of meter for measurement ΔZ using Fabri-Perot interferometer inside the body of test mass (fig. 4) and show that in practice parasitic thermorefractive effect does not allow to control difference ΔZ. This effect consists in thermodynamical fluctuations of temperature which causes fluctuations of refractive index n due to its dependence on temperature T. Due to relatively large value dn/dT for fused silica and sapphire (the more suitable materials for test mass) the readout of meter will give little information about fluctuations of difference ΔZ but mainly about fluctuations of temperature, averaged over volume of meter beam. This scheme of meter for compensation is obvious and we hope that our negative result will be useful for further discussion and investigation on this problem.

For calculation of thermoelastic and Brownian noise of coordinate $Z_{\rm spot}$ we use the results of [4] obtained in approximation of *infinite* test mass.

The Value of Compensation

Using Fluctuation-Dissipation Theorem (FDT) one can calculate spectral density $S_{\rm spot}(\omega)$ of displacement $Z_{\rm spot}$ [10,7,8,4,6]. In this approach one should apply imaginary periodic pressure p distributed over the beam spot on the surface:

$$p(t) = \frac{F_0}{\pi r_0^2}\, e^{-r^2/r_0^2}\, e^{i\omega t} \tag{20}$$

and to calculate the power $W_{\rm loss}$ of losses averaged over period $2\pi/\omega$. Then the spectral density can be determined by formula

$$S_{\rm spot}(\omega) = \frac{8k_{\rm B}TW_{\rm diss}}{F_0^2\omega^2}. \tag{21}$$

One can also calculate separately the spectral density $S_{\rm back}(\omega)$. It is naturally to define coefficient K of relative compensation as the following

$$K_{\rm comp} = \sqrt{\frac{S_{\rm spot}(\omega)}{S_{\rm back}(\omega)}}. \tag{22}$$

It is also useful to compare the spectral density $S_{\rm back}(\omega)$ with the spectral density corresponding to SQL (which is planned to approach in LIGO II) and calculate the coefficient (see [4,9]):

$$K_{\rm SQL} = \sqrt{\frac{S^{\rm SQL}(\omega)}{S_{\rm back}(\omega)}} = \sqrt{\frac{4\hbar}{m\omega^2 S_{\rm back}(\omega)}}, \tag{23}$$

where $\hbar$ is Plank constant and m is the mass of test body. Below we consider thermoelastic and Brownian noises.

Thermoelastic noise

Using results of [4] one can write down the expression for spectral density of thermoelastic noise of spot for infinite test mass:

$$S^{\rm TE}_{\rm spot}(\omega) = \frac{8}{\sqrt{2\pi}}\,\frac{\kappa T^2\alpha^2(1+\sigma)^2\,\lambda^*}{(\rho C)^2\,r_0^3\,\omega^2}. \tag{24}$$

Here κ is Botzmann constant, T is temperature, α is coefficient of thermal expansion, σ is Poison ratio, λ^* is thermal conductivity, ρ is density and C is specific heat capacity. This formula is valid in adiabatic approximation

$$\frac{(\rho C)r_0^2\omega}{\lambda^*} \gg 1 \tag{25}$$

which takes place for parameters of possible materials for test mass in LIGO.

Using FDT approach one can calculate the similar expression for spectral density of thermoelastic noise for back wall (see Appendix D1):

$$S^{\rm TE}_{\rm back}(\omega) = \frac{4\alpha^2\kappa T^2\lambda^*}{\pi\,(\rho C)^2\,R^2 H\,\omega^2}, \tag{26}$$

and calculate the coefficients for thermoelastic noise:

$$K^{\rm TE}_{\rm comp} = \sqrt{\frac{S^{\rm TE}_{\rm spot}(\omega)}{S^{\rm TE}_{\rm back}(\omega)}} = \sqrt{\frac{\sqrt{2\pi}\,(1+\sigma)^2 R^2 H}{r_0^3}}, \tag{27}$$

$$K^{\rm TE}_{\rm SQL} = \sqrt{\frac{S^{\rm SQL}(\omega)}{S^{\rm TE}_{\rm back}(\omega)}} = \sqrt{\frac{\pi\,\hbar(\rho C)^2\,R^2 H}{\alpha^2\kappa T^2 m\lambda^*}} = $$

$$= \sqrt{\frac{\hbar\rho C^2}{\alpha^2\kappa T^2\lambda^*}}. \tag{28}$$

In last equality we used that $m = \pi\,\rho\,R^2 H$.

Brownian noise

The spectral density of Brownian noise for infinite test mass was obtained in [8,4,6] using FDT:

$$S^{\rm B}_{\rm spot}(\omega) = \frac{4\kappa T}{\omega}\,\frac{(1-\sigma^2)}{\sqrt{2\pi}Er_0}\,\phi, \tag{29}$$

where E is Young modulus, ϕ is loss angle.

Using FDT one can calculate the similar expression for spectral density of Brownian noise for back wall (see Appendix D2) and coefficients $K_{\rm comp}$ and $K_{\rm SQL}$:

$$S^{\rm B}_{\rm back}(\omega) = \frac{4\kappa T}{\omega}\,\frac{H}{3\pi E R^2}\,\phi, \tag{30}$$

$$K^{\rm B}_{\rm comp} = \sqrt{\frac{S^{\rm B}_{\rm spot}(\omega)}{S^{\rm B}_{\rm back}(\omega)}} = \sqrt{\frac{3\sqrt{\pi}\,(1-\sigma^2)R^2}{\sqrt{2}\,r_0 H}}, \tag{31}$$

$$K^{\rm B}_{\rm SQL} = \sqrt{\frac{S^{\rm SQL}_{\omega}}{S^{\rm B}_{\rm back}(\omega)}} = \sqrt{\frac{\hbar}{\kappa T}\,\frac{3\pi E R^2}{mH\omega\,\phi}} = $$

$$= \sqrt{\frac{\hbar}{\kappa T}\,\frac{3E}{\rho H^2\omega\,\phi}}. \tag{32}$$

Numerical Estimates

We use the same numerical values of parameters as in [4]:

$$\omega = 2\pi \times 100 \text{ s}^{-1}, \quad T = 300 \text{ K}. \tag{33}$$

Fused silica (SiO_2) :

$$\alpha = 5.5 \times 10^{-7} \text{ K}^{-1}, \quad \rho = 2.2 \text{ g/cm}^3, \tag{34}$$

$$\lambda^* = 1.4 \times 10^5 \text{ erg/(cm s K)},$$

$$C = 6.7 \times 10^6 \text{ erg/(g K)},$$

$$m = 1.1 \times 10^4 \text{ g}, \quad R = 12.5 \text{ cm},$$

$$H = 10.2 \text{ cm}, \quad \phi = 5 \times 10^{-8},$$

$$E = 7.2 \times 10^{11} \text{ erg/cm}^3, \quad \sigma = 0.17,$$

$$\beta = \frac{1}{n}\left(\frac{dn}{dT}\right) = 1 \times 10^{-5} \text{ K}^{-1}.$$

Sapphire (Al_2O_3) :

$$\alpha = 5.0 \times 10^{-6} \text{ K}^{-1}, \quad \rho = 4.0 \text{ g/cm}^3 \tag{35}$$

$$\lambda^* = 4.0 \times 10^6 \text{ erg/(cm s K)},$$

$$C = 7.9 \times 10^6 \text{ erg/(g K)},$$

$$m = 3 \times 10^4 \text{ g}, \quad R = 14.0 \text{ cm},$$

$$H = 12.2 \text{ cm}, \quad \phi = 3 \times 10^{-9},$$

$$E = 4 \times 10^{12} \text{ erg/cm}^3, \quad \sigma = 0.29,$$

$$\beta = \frac{1}{n}\left(\frac{dn}{dT}\right) = 0.7 \times 10^{-5} \text{ K}^{-1}.$$

For these parameters one can obtain the estimates given in table I.

From table I one can see that SQL can be overcome by 2.7 times for fused silica and by 3.9 times for sapphire. It is also natural that thermoelastic noise dominating in sapphire can be easier compensated due to its more strong dependence on spot radius r_0 (compare (24) and (29)).

Interferometric Compensation Meter

One of possible meters for independent control of averaged coordinate of spot $Z_{\rm spot}$ on test mass surface is shown on fig. (4). Several Fabri-Perot interferometers are necessary in order to gather information on possible larger surface of back wall. It is difficult to use beam with radius r_{00} more than several millimeters (in opposite case the interferometer mode became unstable). Therefore several dozens of inner interferometric beams must be used. Let us assume that experimentalist have possibility to create such device.

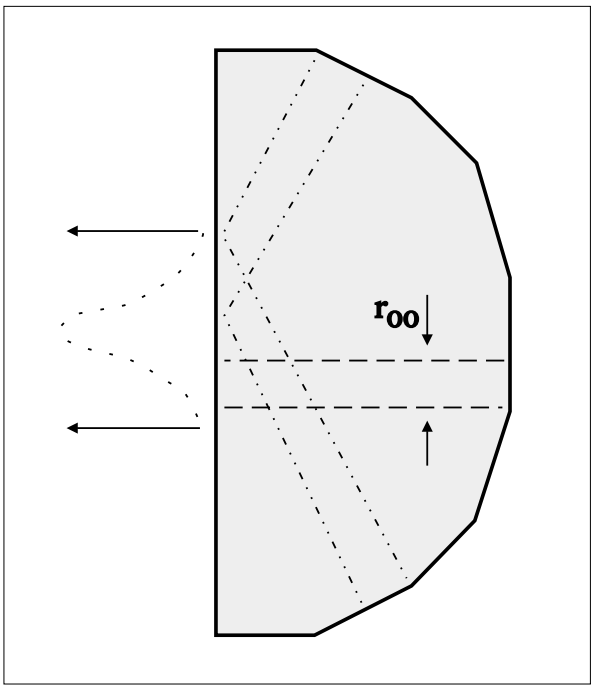

FIG. 4. Interferometric meter for independent control of averaged coordinate of laser spot (on left side of test mass), consisting of several Fabri-Perot interferometers placed inside test mass. Only two inner interferometer beams are shown.

Having analyzed this meter we found that parasitic thermorefractive effect plays an important role. This effect consists in thermodynamical fluctuations of temperature T which causes fluctuations of refractive index n of test mass body due to its dependence on temperature (nonzero coefficient dn/dT) and consequently leads to phase fluctuations of wave propagating in interferometer. Indeed the phase φ of output beam, for example, of central

interferometer (on fig. 4 its beam is horizontal) will take out information about sum:

$$\varphi \sim n(Z_{\mathrm{F.spot}} - Z_{\mathrm{B.spot}}) + H\,\frac{dn}{dT}\,\Delta T, \tag{36}$$

where $Z_{\mathrm{F.spot}}$ and $Z_{\mathrm{B.spot}}$ are averaged coordinates on face and back surfaces of test mass correspondingly (averaging over crossection is made with weight gaussian function: $\frac{1}{\pi r_{00}^2}\,e^{-r^2/r_{00}^2}$), H is the width of test mass, ΔT is thermodynamical fluctuations of temperature averaged over beam volume. Using natural condition $r_{00} > H$ we also assume that fluctuations of $Z_{\mathrm{F.spot}}$ and $Z_{\mathrm{B.spot}}$ are not correlated. Then the value of parasitic influence of thermorefractive effect can be estimated by coefficient:

$$A_{\mathrm{TR}} = \sqrt{\frac{2}{(H\beta)^2}\frac{S_{\mathrm{spot}}}{S_{\mathrm{TD}}}}, \qquad \beta = \frac{1}{n}\left(\frac{dn}{dT}\right). \tag{37}$$

Here S_{spot} is the spectral density of beam spot, expressed by formulas (24, 29) for thermoelastic and Brownian noise correspondingly, and S_{TD} is the spectral density of thermodynamical fluctuations of temperature averaged over beam volume. The last spectral density can be calculated using the model of infinite layer with width H in order not to account the boundary condition on lateral area.

For calculation the thermodynamical fluctuations of temperature $u(\vec{r},t)$ one can use Lahgevin approach and introduce fluctuational thermal sources $F(\vec{r},t)$ added to the right part of the equation of thermal conductivity [4]:

$$\frac{\partial u}{\partial t} - \frac{\lambda^*}{\rho C}\,\Delta u = F(\vec{r},t), \tag{38}$$

$$\langle\, F(\vec{r},t)F(\vec{r}',t')\,\rangle = -F_0^2\,\Delta\delta(\vec{r}-\vec{r}')\,\delta(t-t'), \tag{39}$$

$$F_0^2 = 2\frac{\kappa T^2\lambda^*}{(\rho C)^2},$$

where Δ is Laplace operator, $\delta(\vec{r})$ and $\delta(t)$ are spatial and time delta-functions correspondingly. As a result one can obtain formula for spectral density S_{TD} of thermodynamical fluctuations of temperature averaged over beam volume (see Appendix D3):

$$S_{\mathrm{TD}}(\omega) = 2\,\frac{\kappa T^2\lambda^*}{(\rho C)^2 H}\,\frac{1}{\pi r_{00}^4\omega^2}. \tag{40}$$

The expressions for coefficients $A_{\rm TR}$ for thermoelastic and Brownian noises can be obtained using (24,29,37):

$$A_{\rm TR}^{\rm TE} = (1+\sigma)\,\frac{\alpha}{\beta}\,\sqrt{4\sqrt{2\pi}\,\frac{r_{00}}{H}}, \tag{41}$$

$$A_{\rm TR}^{\rm B} = \sqrt{\frac{4\sqrt{2\pi}\,(1-\sigma^2)(\rho C)^2\phi\omega r_{00}^3}{T\lambda^* EH\beta^2}}.$$

In table II the numerical estimates for these coefficients are given. All coefficients $A_{\rm TR}$ are much less than unity. This means that thermorefractive effect strongly masks the useful information about fluctuations of averaged coordinate of laser spot on test mass surface.

TABLES

TABLE I. Coefficients $K_{\rm comp}$ (22) and $K_{\rm SQL}$ (23) for thermoelastic noise (superscript $^{\rm TE}$) and for Brownian noise (superscript $^{\rm B}$) for fused silica and sapphire using parameters (33,34,35).

	Fused silica		Sapphire	
r_0 (cm)	1.5	3.0	1.5	3.0
$K^{\rm TE}_{\rm comp}$	40.2	14.2	54.3	19.2
$K^{\rm B}_{\rm comp}$	5.1	3.6	4.5	3.2
$K^{\rm TE}_{\rm SQL}$	430.2		14.1	
$K^{\rm B}_{\rm SQL}$	2.7		3.9	

TABLE II. The coefficients $A_{\rm TR}$ for thermoelastic noise (superscript $^{\rm TE}$) and for Brownian noise (superscript $^{\rm B}$) for fused silica and sapphire using parameters (33,34,35).

	Fused silica	
r_{00}	0.15 cm	0.30 cm
$A^{\rm TE}_{\rm TR}$	0.024	0.034
$A^{\rm B}_{\rm TR}$	0.051	0.14
	Sapphire	
r_{00}	0.15 cm	0.30 cm
$A^{\rm TE}_{\rm TR}$	0.32	0.46
$A^{\rm B}_{\rm TR}$	0.01	0.027

Conclusion

As we said in Introduction the results of section II collected table I reflect the extreme optimistic points of view. Unfortunately nobody knows how to realize such compensation measurement. In section II we demonstrate that parasitic thermorefractive effect happens to be considerable value and it prevents from considered design of "inner" compensation meter.

One of the alternatives way is to construct device controlling the distance between laser spot on test mass and averaged coordinate of *additional* support body. In this case one can create many beams inteferometer, but thermorefractive effect will not make difficulties because each beam can propagate in free space. However the problem of high quality suspension of additional body with mass not less than test mass is a separate and rather complicated experimental one.

Appendix D1. Thermoelastic Noise

In this appendix we calculate the formula (26).

In according to FDT one must apply force F_0 alternating with frequency ω which is homogeneously distributed over cylinder base (i.e. it makes the constant pressure $F_0/\pi R^2$) and calculate the value of losses averaged over the period. Therefore we must solve the system of equations of elasticity and thermoconductivity:

$$\frac{(1-\sigma)}{(1+\sigma)}\mathbf{grad\ div}\ \vec{v} - \frac{1-2\sigma}{2(1+\sigma)}\mathbf{rot\ rot}\ \vec{v} = \tag{42}$$
$$\vec{e}_z\,\frac{F_0(1-2\sigma)}{\pi R^2 H\,E} + \alpha\,\vec{\nabla}\delta T,$$

$$\sigma_{zz}|_{z=H} = \frac{E}{1-2\sigma}\,\alpha\,\delta T|_{z=H}, \tag{43}$$
$$\sigma_{zz}|_{z=0} = -\frac{F_0}{\pi R^2} + \frac{E}{1-2\sigma}\,\alpha\,\delta T|_{z=0},$$
$$\sigma_{zr}|_{z=0,\,H} = 0, \qquad \sigma_{zr}|_{r=R} = 0$$
$$\sigma_{rr}|_{r=R} = \frac{E}{1-2\sigma}\,\alpha\,\delta T|_{r=R}, \tag{44}$$

$$\frac{\partial \delta T}{\partial t} - a^2 \Delta \delta T = -\frac{\alpha\, ET}{C\rho(1-2\sigma)} \frac{\partial\, \mathbf{div}\, \vec{v}}{\partial t}, \tag{45}$$

$$a^2 = \frac{\lambda^*}{\rho C},$$

$$\left.\frac{\partial \delta T}{\partial z}\right|_{z=0,\,H} = 0, \qquad \left.\frac{\partial \delta T}{\partial r}\right|_{r=R} = 0.$$

Zero Approximation

We solve this system by method of perturbation. In zero approximation we find field of deformation $\vec{v}_0$ formally putting $\alpha = 0$. The solution for vector of displacement $\vec{v}_0$ of this problem is known (we go into noninertial system and face the problem for cylinder in field of artificial gravity — see e.g. sec. 1.7 in [10]):

$$v_{0z} = \frac{F_0}{\pi r^2\, E} \left(\frac{\sigma\, r^2}{2H} - z + \frac{z^2}{2H} \right), \tag{46}$$

$$v_{0r} = \frac{F_0}{\pi r^2\, E} \frac{\sigma r}{H} \left(1 - \frac{z}{H} \right), \tag{47}$$

$$\mathbf{div}\, \vec{v} = -\frac{F_0(1-2\sigma)}{\pi R^2 E} \left(1 - \frac{z}{H} \right). \tag{48}$$

The axis of cylindrical system of coordinate coincides with axis of cylinder and bases of cylinder have coordinates $z = 0,\, H$.

it First Approximation

Substituting $\vec{v}_0$ in the right part of equation (45) we find the temperature field δT_1, appearing due to elastic deformations (it is the first approximation proportional to $\sim \alpha$). We are to solve the following problem in two steps:

$$i\omega\, \delta T_1 - a^2 \Delta \delta T_1 = -\frac{\alpha\, ET}{C_V \rho(1-2\sigma)}\, i\omega\, \mathbf{div}\, \vec{v}_0$$

$$\left.\frac{\partial \delta T_1}{\partial z}\right|_{z=0,\,H} = 0, \quad \left.\frac{\partial \delta T_1}{\partial r}\right|_{r=R} = 0,$$

$$\delta T_1 = -\frac{\alpha\, ET}{C_V \rho(1-2\sigma)}\, \mathbf{div}\, \vec{v}_0 + \delta \tilde{T}_1,$$

$$i\omega\, \delta \tilde{T}_1 - a^2 \Delta \delta \tilde{T}_1 = 0,$$

$$\left.\frac{\partial \delta \tilde{T}_1}{\partial z}\right|_{z=0,\,H} = \frac{\alpha\, ET}{C_V \rho(1-2\sigma)} \left.\frac{\partial \mathbf{div}\, \vec{v}_0}{\partial z}\right|_{z=0,\,H},$$

$$\left.\frac{\partial \delta\tilde{T}_1}{\partial r}\right|_{r=R} = \frac{\alpha\, ET}{C_V \rho(1-2\sigma)} \left.\frac{\partial \mathbf{div}\, \vec{v}_0}{\partial r}\right|_{r=R} = 0.$$

The solution for $\delta\tilde{T}_1$ can be found in the following form:

$$\delta\tilde{T}_1 = \frac{F_0\, \alpha\, T}{\pi R^2 C_V \rho} \left(D_0 e^{s_0 z} + G_0 e^{-s_0 z}\right),$$
$$D_0 = \frac{e^{-s_0 H}}{s_0 H\,(1+e^{-s_0 H})}, \qquad s_0 = \frac{\sqrt{i\omega}}{a},$$
$$G_0 = -\frac{1}{s_0 H\,(1+e^{-s_0 H})}.$$

Let us calculate auxilary dimentionless integral, which will be used below.

$$I_0 = \frac{1}{H}\int_0^H dz\, \left(D_0 e^{s_0 z} + G_0 e^{-s_m z}\right) \left(-1+\frac{z}{H}\right) =$$
$$= \frac{1}{(s_0 H)^2} \left[1 - \frac{2\left(1-e^{-s_0 H}\right)}{s_0 H\,(1+e^{-s_0 H})}\right] \simeq \frac{1}{(s_0 H)^2}. \qquad (49)$$

In last equality we use condition $|s_0 H| \gg 1$.

Second Approximation

Now one can substitute $\vec{\nabla}\delta T_1$ in the right part of equation (42). Then in principle one can find the second approximation $\vec{v}_2$ to the field of deformations (it is proportional to $\sim \alpha^2$) and then after extraction of imaginary part of $\vec{v}_2$ it is possible to find energy of losses $\mathcal{E}_{\rm loss}$ per period.

However we have the possibility to make calculation procedure much easier and not to sovle elastic problem for $\vec{v}_2$. Note that right part in (42) is iquivalent to volume force

$$\vec{f}_2 = -\frac{E}{(1-2\sigma)}\, \alpha\, \vec{\nabla}\, \delta T_1.$$

Plus we have pressure

$$\vec{p}_2 = \frac{E}{(1-2\sigma)}\, \alpha\, \delta T_1\, \vec{n},$$

acting normally to surface of cylinder ($\vec{n}$ is external unit normal, see (42 - 44)). The imaginary parts of $\vec{f}_2$ and $\vec{p}_2$ are the small forces of friction and one can find power $W_{\rm diss}$ of losses by calculation the power of these forces:

$$W_{\rm diss} = -\frac{\omega}{2}\,\Im\left(\int_V dV\,(\vec{v}_0\cdot\vec{f}_2) + \int_S dS\,(\vec{v}_0\vec{p}_2)\right) =$$
$$= -\frac{\omega\alpha E}{2(1-2\sigma)}\,\Im\left(\int_V dV\,\mathbf{div}\,\vec{v}_0\,\delta\tilde{T}_1\right) =$$
$$= -\frac{2F_0^2(1+\sigma)^2\omega\alpha^2 T}{C_V\rho}\,\frac{H}{\pi R^2}\,\Im\left(I_0\right). \qquad (50)$$

Substituting (50) into (21) we obtain the formula (26).

Appendix D2. Brownian noise

In this Appendix we calculate the formula (30).

Using formulas for displacement vector $\vec{v}_0$ obtained in Appendix II one can calculate elastic energy $\mathcal{E}$ as work, performed by volume and surface forces:

$$\mathcal{E} = \mathcal{E}_f + \mathcal{E}_F.$$
$$\mathcal{E}_f = \frac{1}{2}\int_{-H/2}^{H/2} dz \int_0^R 2\pi\, r\, dr\,\frac{F_0}{\pi R^2 H}\,v_{0z} =$$
$$= \frac{F_0^2 H}{\pi R^2 E}\left(\frac{1}{6} - \frac{\sigma R^2}{8H^2}\right),$$
$$\mathcal{E}_F = -\frac{1}{2}\int_0^R 2\pi\, r\, dr\,\frac{F_0}{\pi R^2} v_{0z}|_{z=H/2} =$$
$$= \frac{F_0^2 H}{\pi R^2 E}\,\frac{\sigma R^2}{8H^2},$$
$$\mathcal{E} = \frac{F_0^2 H}{6\pi R^2 E}. \qquad (51)$$

Then assuming that $W_{\rm diss} = \mathcal{E}\omega\phi$ and substituting it for (21) one can obtain (30).

Appendix D3. TD fluctuations of temperature

In this Appendix we calculate the formula (40).

The TD fluctuations of temperature $u(\vec{r},t)$ one can find in spectral form:

$$u(\vec{r},t) = \iiint_{-\infty}^{\infty}\frac{dk_x dk_y d\omega}{(2\pi)^3}\times$$
$$\times\sum_n u_n(k_x,k_y,\omega)e^{i\omega t - ik_x x - ik_y y}\,\cos b_n z,$$

$$u_n(k_x,k_y,\omega)=\frac{F_n(k_x,k_y,\omega)}{i\omega+a^2(b_n^2+k_\perp^2)},$$
$$k_\perp^2=k_x^2+k_y^2,\quad b_n=\frac{\pi n}{H}.$$

Using (39) one can find correlators of spectral expantion of the fluctuational thermal sourses:

$$\langle\, F_n(k_x,k_y,\omega)F_{n_1}^*(k_{x_1},k_{y_1},\omega_1)\,\rangle=\frac{2\kappa T^2\lambda^*}{(\rho C)^2}(2\pi)^3\times \tag{52}$$
$$\times\left(k_\perp^2+b_n^2\right)\frac{2}{l}\delta_{n,n_1}\delta(k_x-k_{x_1})\times\delta(k_y-k_{y_1})\,\delta(\omega-\omega_1)$$

Now one can calculate the spectral density $S_{\bar u}(\omega)$ of fluctuations of temperature $\bar u(t)$, averaged over volume $V=\pi r_{00}^2H$ along axis z:

$$\bar u(t)=\frac{1}{\pi r_{00}^2H}\int_0^H dz\iint_0^\infty dx\,dy\,u(\vec r,t)e^{-\frac{x^2+y^2}{r_{00}^2}},$$
$$S_{\bar u}(\omega)=\frac{2\kappa T^2\lambda^*}{(\rho C)^2H}\int\int_{-\infty}^{\infty}\frac{dk_xdk_y}{(2\pi)^2}\,e^{-\frac{r_{00}^2k_\perp}{2}}\frac{k_\perp^2}{\omega^2+a^4k_\perp^4}=$$
$$=\frac{2\kappa T^2\lambda^*}{(\rho C)^2H}\int_0^\infty\frac{k_\perp dk_\perp}{2\pi}\,e^{-\frac{r_{00}^2k_\perp}{2}}\frac{k_\perp^2}{\omega^2+a^4k_\perp^4}\simeq$$
$$\simeq\frac{2\kappa T^2\lambda^*}{(\rho C)^2H}\,\frac{1}{\pi r_{00}^4\omega^2}. \tag{53}$$

The last expression, obtained in adiabatic approximation $(\omega r_{00})/a^2\gg 1$, obviously coincides with (40).

REFERENCES

[1] A. Abramovici *et al.*, *Science* **256** (1992) 325.

[2] A. Abramovici *et al.*, *Physics Letters* **A218**, 157 (1996).

[3] V. B. Braginsky, M. L. Gorodetsky and S. P. Vyatchanin, *Physics Letters A*, **A264**, 1 (1999).

[4] Yu. T. Liu and K. S. Thorne, submited to Phys. Rev. D (available in archive xxx.lanl.gov: gr-qc/0002055)

[5] V. B. Braginsky, Yu. Levin and S. P. Vyatchanin, *Meas. Sci. Technol.*, **10**, 598 (1999).

[6] P. R. Saulson, *Rhys. Rev. D*, **42**, 2437 (1990);
G. I. Gonzalez and P. R. Saulson, *J. Acoust. Soc. Am.*, **96**, 207 (1994).

[7] Yu. Levin, *Phys. Rev. D*, **57**, 659-663 (1998).

[8] F. Bondu, P. Hello, Jean-Yves Vinet, *Physics Letters* **A 246**, 227 (1998).

[9] V. B. Braginsky, M. L, Gorodetsky, F. Ya. Khalili and K. S. Thorne, *Report at Third Amaldi Conference, Caltech*, July, 1999.

[10] L. D. Landau and E. M. Lifshitz, *Theory of Elasticity*, third edition (Pergamon, Oxford, 1986).

Appendix E. On the possibility to measure thermo-refractive noise in microspheres

Introduction

Optical microresonators with whispering gallery modes when made of pure fused silica have a unique combination of high quality factor (of the order of 10^{10}) and small size (hundreds of microns) [1–3]. These features in combination with ease of production naturally lead to the usage of these resonators as external cavities for diode laser stabilization, discriminators and passive filters. However very small size of resonators have the drawback. It is shown below that thermodynamical fluctuations of temperature in the mode-volume of the resonators may not be neglected. These fluctuations lead due to thermal dependence of refractive index to its fluctuations and hence to the trembling of the resonance frequency and depending on the tuning to phase or amplitude noise of the output light-wave. This effect is different and uncorrelated with the known effect of thermodynamical fluctuation of density leading to Rayleigh scattering.

The effect of thermodynamical fluctuations of temperature in the bulk of the mirrors on the sensitivity of Fabry-Perot etalon was analyzed for the first time in [4]. The thermodynamical fluctuations of temperature in this case are acting in two ways 1) due to coefficient of thermal expansion they produce fluctuations of the surfaces of the mirrors (thermoelastic noise); 2) due to coefficient of thermal refraction they produce fluctuations of phase in the wave reflected from multilayer coating which may also be recalculated to the equivalent fluctuations of the surface (thermo-refractive noise). It was shown that these effects will restrict the sensitivity of laser gravitational wave antenna [6] that are being constructed now and should be seriously taken into account on the next stages of this project.

The idea of the effect follows from the well known thermodynamical equation for the variance of temperature fluctuation u in the volume V:

$$\langle u^2 \rangle = \frac{\kappa T^2}{\rho C V}, \tag{54}$$

where T is temperature of the heat-bath, κ is the Boltzmann constant, ρ is density, and

C specific heat capacity. By substituting in this equation parameters for fused silica $\rho = 2.2$ g/cm^3, $C = 6.7 \times 10^6$ erg/(g K) and effective volume of field localization of the most localized mode in the microsphere with $V \simeq 10^{-9}$ cm^3 we obtain the value of $\sqrt{\langle u^2 \rangle} \simeq 30\,\mu$K which in combination with the coefficient of thermal refraction $dn/dT = 1.45 \times 10^{-5}\ K^{-1}$ lead to rather pronounced effect of relative resonance frequency fluctuations $\delta\omega/\omega \sim 3 \times 10^{-9}$. This value is even larger than the linewidthes of resonances achievable in microspheres. I shall not analyze thermoelastic noise here, as the coefficient of thermal expansion $\alpha = 5.5 \times 10^{-7}$ K^{-1} is sufficiently smaller in fused silica than dn/dT.

It is evident, however, that to find spectral properties of this noise, more rigorous analysis is required, taking into account peculiar field distribution of whispering gallery modes.

Thermodynamical fluctuations of temperature

In [4,5] the new approach for the analysis of thermodynamical fluctuations of temperature was developed - the method of fluctuational fluctuational thermal sources $F(\vec{r}, t)$ substituted to the right part of the equation of thermal conductivity

$$\frac{\partial u}{\partial t} - a^2 \Delta u = F(\vec{r}, t), \tag{55}$$

where $a^2 = \lambda^*/(\rho C)$ and λ^* is thermal conductivity. This approach is analogous to the Langevin approach with fluctuational forces in equations of dynamics. It was shown that if the proper normalization of the sources is used:

$$\langle F(\vec{r}, t) F(\vec{r}', t') \rangle = \frac{2\kappa T^2 a^2}{\rho C} \nabla^2 \delta(\vec{r} - \vec{r}') \delta(t - t'), \tag{56}$$

this approach leads to correct results which satisfy Fluctuation-Dissipation theorem (FDT). In particular it was shown that thermoelastic noise is associated through FDT with thermoelastic damping.

Simple estimate of the spectrum of fluctuations in microspheres

Variations of refractive index n in dielectric cavity lead to the change of resonance frequencies. To find this change one may use variational approach. If the perturbed wave-equation has the form:

$$\Delta\vec{E} + \frac{\epsilon^0 + 2n\delta n}{c^2}\omega^2\vec{E} = 0, \tag{57}$$

Where $\vec{E}$ is the electric field in the cavity, $\epsilon^0 = n^2$ is dielectric susceptibility, $\delta n = \frac{dn}{dT}u$ is the variation of refractive index due to fluctuations of temperature u. If $\vec{E}_0$ is the orthonormalized field distribution of an eigenmode of the unperturbed cavity ($\int \vec{E}_i\vec{E}_j^*d\vec{r} = \delta_{ij}$) and $\omega = \omega_0 + \delta\omega$ is the frequency shift, then after multiplication of this vector equation on complex conjugate vector $\vec{E}_0^*$ and integration over the whole volume, neglecting the terms of the second order we obtain:

$$\frac{\delta\omega}{\omega_0} = -\frac{1}{n}\int\limits_V |\vec{E}_0^2|\delta n d\vec{r} = -\frac{1}{n}\frac{dn}{dT}\bar{u}, \tag{58}$$

where u is the temperature deviation averaged over the mode volume. For simplicity of calculations below I restrict myself with only fundamental whispering-gallery mode $TE_{\ell\ell 1}$ in microspheres of radius R, which has the smallest volume of localization. The field distribution of this mode may be approximated as follows:

$$\vec{\mathbf{E}}(r,\theta,\phi) \simeq \vec{\mathbf{E}}_\theta(r,\theta,\phi) \simeq$$
$$\frac{4(\pi\ell)^{1/4}}{n\sqrt{n^2-1}a^{3/2}}e^{-\ell\cos^2\theta/2+i\ell\phi}\begin{cases} \mathrm{j}_\ell(knr)/\mathrm{j}_\ell(knR) \text{ for } r \le R \\ e^{-\gamma(r-R)} \text{ for } r > R \end{cases},$$
$$knR \simeq \ell + 1/2 + 1.8558(\ell+1/2)^{1/3} - \frac{n}{\sqrt{n^2-1}} \tag{59}$$

However, even this approximation is too complex for further evaluation, so below I shall use the following Gaussian approximation of radial dependence:

$$\hat{\mathbf{e}}_\theta(r,\theta,\phi) \simeq \frac{\ell^{1/4}}{\pi\sqrt{2b}R_0}e^{-\frac{(r-R_0)^2}{2b^2}-\frac{\ell\cos^2\theta/2}{2}+i\ell\phi}$$
$$knR_0 \simeq \ell + 1/2 + 0.71(\ell+1/2)^{1/3}$$
$$knb \simeq 0.81(\ell+1/2)^{1/3}. \tag{60}$$

This approximation describes rather adequately the distribution of optical energy inside the resonator. Moreover as it will be found below because of the small depth of the field (parameter b, radial distribution practically does not influence on the frequency fluctuations.

It is now necessary to calculate thermodynamical fluctuations of temperature in the sphere. In [5] the spectral density of these fluctuations near the boundary of half-space was found:

$$u(\vec{r},t) = \int\limits_{-\infty}^{\infty} \frac{F(\vec{\beta},\Omega)}{a^2\beta^2 + i\Omega} e^{i\Omega t + i\vec{\beta}\vec{r}} \frac{d\vec{\beta}\, d\Omega}{(2\pi)^4}$$

$$\langle\, F(\vec{\beta},\Omega) F^*(\vec{\beta}',\Omega')\,\rangle = (2\pi)^4 \frac{2a^2\kappa T^2}{\rho C} \beta^2 [\delta(\beta_\perp - \beta'_\perp) + \delta(\beta_\perp + \beta'_\perp)]\, \delta(\vec{\beta}_{||} - \vec{\beta}'_{||})\, \delta(\Omega - \Omega'), \quad (61)$$

where $\beta_\perp$ is the component of wave-vector of fluctuations normal to the surface and $\vec{\beta}_{||}$ are components, parallel to it, $a^2 = \lambda^*/(\rho C)$, and λ^* is thermal conductivity.

We may use this result for the evaluations by putting $\beta_\perp = \beta_r$ as we are interested in the fluctuations near the surface of the microsphere and the relaxation time of the whole microsphere $\tau_T \sim R^2/a^2 \geq 2.5\,\mathrm{ms}$ (for $R \geq 50$ μm is much longer than the usual times of interest.

Rigorous integration in spherical coordinates is rather complex here, so . for the first estimate one may significantly simplify the problem by introducing local orthogonal coordinates near the surface with axes z normal to the surface, axes y orthogonal to the equatorial plane and x, normal to it. The whole torus of the mode near the surface of the sphere is substituted in this approach by a stripe under the surface of the half-space:

$$\hat{\mathbf{e}}_y(x,y,z) \simeq \frac{\ell^{1/4}}{\pi\sqrt{2b}R_0} e^{-\frac{(z-z_0)^2}{2b^2} - \frac{x^2}{2d^2} - \frac{y^2}{2w^2}}$$

$$d = R_0/\sqrt{\ell} \quad knz_0 \simeq 1.14(\ell + 1/2)^{1/3} \quad w \simeq \sqrt{2}\pi R_0 \qquad (62)$$

The thermodynamical fluctuations of temperature $\bar{u}$ averaged over the volume $V = 2\pi^2 Rdb$ may be presented in the following form:

$$\bar{u} = \frac{1}{V} \int\limits_0^{\infty} \int\limits_{-\infty}^{\infty} \int\limits_{-\infty}^{\infty} u(\vec{r},t)\; e^{-x^2/w^2} e^{-y^2/d^2} e^{-(z-b)^2/l^2} dz dx dy$$

$$\simeq \int\limits_{-\infty}^{\infty} \frac{d\vec{k}\, d\omega}{(2\pi)^4} \frac{F(\vec{k},\omega) e^{i\omega t}}{a^2|\vec{k}|^2 + i\omega} e^{-k_x^2 w^2/4} e^{-k_y^2 d^2/4} e^{-k_z^2 b^2/4} \qquad (63)$$

Now we may calculate the following averaged value $B(\tau) = \langle u(t)u(t+\tau)\rangle$ and (correlation function of relative frequency fluctuations) and from Wiener-Hinchin theorem the one-sided (hence additional factor 2) spectral density $S^2_{\delta\omega/\omega}(\Omega)$ of relative fluctuations of frequency in this approach:

$$S^2_{\delta\omega/\omega}(\Omega) \simeq \frac{4a^2\kappa T^2}{n^2\rho C}\left(\frac{d\,n}{d\,T}\right)^2 \int_{-\infty}^{\infty}\int_{-\infty}^{\infty}\int_{-\infty}^{\infty} \frac{\beta^2(1+e^{2i\beta_z z_0})}{a^4\beta^4+\Omega^2} e^{-\beta_x^2 w^2/2-\beta_y^2 d^2/2-\beta_z^2 b^2/2}\frac{d\beta_x d\beta_y d\beta_z}{(2\pi)^3} \quad (64)$$

As $w \gg d \gg b$ and due to the exponents, the components of wave-vector adding to the integral, satisfy the condition: $\beta_z \gg \beta_y \gg \beta_x$ and $\beta_x, \beta_y \ll \sqrt{\omega}/a$ we may neglect the term $e^{-\beta_z^2 b^2/2}$. If $\sqrt{\Omega} z_0/a \ll 1$. In this way we may also substitute complex exponent by unity:

$$\int_{-\infty}^{\infty}\frac{d\beta_z}{2\pi}\frac{\beta_z^2}{a^4\beta_z^4+\Omega^2} \simeq \frac{\sqrt{2}}{4a^3\sqrt{\Omega}} \quad (65)$$

$$S^2_{\delta\omega/\omega}(\Omega) = \frac{\kappa T^2\sqrt{\ell}}{\pi^2 n^2 R^2\sqrt{\lambda^*\rho C\Omega}}\left(\frac{d\,n}{d\,T}\right)^2 \quad (66)$$

Substituting these parameters we obtain for the resonator at $\lambda = 0.63\mu m$:

$$S_{\delta\omega/\omega}(\Omega) \simeq 10^{-11}\left(\frac{50\mu m}{R}\right)^{3/4}\left(\frac{1000 s^{-1}}{\Omega}\right)^{1/4}\frac{1}{\sqrt{Hz}} \quad (67)$$

This estimate should be valid for the range of frequencies $10^3 s^{-1} < \Omega < 10^5 s^{-1}$. Comparing this estimate with the quality factors already achieved in microspheres $Q \sim 10^9 \div 10^{10}$ we see, that this value may be measured, and on the slope of the resonance curve the fluctuations of the output power in the narrow band of several Hertz may reach several percents ($\delta W/W = Q\delta\omega/\omega$).

In order this noise could be registered, it should dominate other noises. The fundamental limitation here is the shot noise of laser with spectral density of fluctuations of power $S^2_W = \hbar\omega W$, W is the power of optical light, registered on the detector. However, from the estimate

$$W > \frac{\hbar\omega}{Q^2 S^2_{\delta\omega/\omega}} \simeq 2\times 10^{-5}\mathrm{erg/s}, \quad (68)$$

where I used a moderate value for microspheres of $Q = 10^8$, it follows that this limitation is absolutely inaccential here. The Schawlow-Townes quantum limit of frequency fluctuations in laser field is also not important here,

$$W > \frac{\hbar\omega}{Q_L^2 S^2_{\delta\omega/\omega}}, \tag{69}$$

even if a laser with cold cavity quality-factor Q_L few orders lower than $Q = 10^8$ is used for measurement.

Summing up, the thermo-refractive noise in microspheres may be registered and estimated if the technical problems associated with appropriate whispering-gallery mode excitation and identification are solved.

REFERENCES

[1] V.B. Braginsky, M.L. Gorodetsky, V.S. Ilchenko, Phys. Lett. **A137**, (1989) 393.

[2] M.L. Gorodetsky, V.S. Ilchenko, A.A. Savchenko, "Ultimate Q of optical microsphere resonators", – Opt. Lett. **21** (1996) 453.

[3] D. W. Vernooy, V. S. Ilchenko, H. Mabuchi, E. W. Streed and H. J. Kimble, Opt. Lett. **23** (1998) 247.

[4] V.B. Braginsky, M.L. Gorodetsky and S.P. Vyatchanin, "Thermodynamical fluctuations and photo-thermal shot noise in gravitational wave antennae", – Phys. Lett. **A264** (1999) 1.

[5] V.B. Braginsky, M.L. Gorodetsky and S.P. Vyatchanin, "Thermo-refractive noise in gravitational wave antennae", – Phys. Lett. **A271** (2000) 303.

[6] A. Abramovici et al., Science **256** (1992) 325.

Appendix F. Frequency fluctuations of nonlinear origin in self-sustained optical oscillators

Introduction

The impressive achievements in quantum optical and spectroscopic experiments during the last two decades in many cases have its origin in the invention and implementation of self-sustained optical oscillators (lasers) with very small frequency fluctuations. The record high accuracy obtained in the comparison of the values of eigen frequencies of two Fabri-Perot optical resonators performed in the gravitational wave antennae prototype [1,2], is reasonable to be mentioned as a good example of such an achievement. The possibility to detect the relative difference between the two eigenfrequencies at the level of $\Delta\omega_0/\omega_0 \simeq 3 \times 10^{-19}$ with averaging time $\tau \simeq 10^{-2}$ sec was demonstrated in this experiment. There is another "source" of achievements in this area of experimental physics: the steady rise of the optical mirrors finesse $\mathcal{F}$. The obtained few years ago value of $\mathcal{F} \simeq 2 \times 10^6$ [3] permits to realize in the table-top experiment an optical Fabri-Perot resonator with the eigenmode quality factor $Q \simeq 10^{13}$. Using this value of Q the Townes limit $\Delta\omega_0/\omega_0 \simeq 1/(Q\sqrt{N})$ "permits" to measure the level of relative frequency fluctuations $\simeq 10^{-21}$ if only $N = 10^{16}$ optical photons will be "spend". It is worth noting that nobody has formulated any fundamental limit for the value of $\mathcal{F}$ yet.

Recently M. L. Gorodetsky together with the authors of this article [4,5] and Yu. T. Liu with K. S. Thorne [6] have analyzed the random deviations of the eigen frequency ω_r of Fabri-Perot resonator produced by thermodynamic fluctuations of temperature T and by the temperature fluctuations appearing due to the random absorption of optical photons in the resonator mirrors. These effects are in essence of nonlinear origin: namely due to thermal expansion, characterized by coefficient $\alpha = \frac{1}{l}\frac{dl}{dT}$, and thermorefractivity (dependence of the refraction index $n(T)$ on temperature T) which can be characterized by coefficient $\beta = \frac{1}{n}\frac{dn}{dT}$). The results presented in these articles show that the thermal fluctuations in the mirrors may

be a serious obstacle when experimentalist wants to reach or even to overcome Standard Quantum Limit (SQL) of frequency.

The goal of this article is to present the results of the analysis of random fluctuations of the frequency in the output radiation of a selfsustained optical oscillator (laser) which are of similar nonlinear origin as in passive Fabri-Perot resonator. All estimates presented in text are given for parameters listed in Appendix F1.

Analyzed Model of Laser

For the analysis we have chosen the laser scheme in which the solid body acts as the amplifying part. The inversion of population in certain optical transition in this solid body is provided by the radiation of the nearby set of photodiodes. One of this laser types (based on Nd:YAG) has a very narrow line width, very high efficiency of photodiode-to-output radiation conversion and high mean output power W (several tens or even hundreds of Watts). The output radiation wavelength mean value in this laser type is $\lambda = 1.06\ \mu$ [7,8]. This laser is being used now in the Laser Interferometer Gravitational wave Observatory (the LIGO project) [1,2,9] in the first stage (LIGO-I) and is planned to be used in the second stage (LIGO-II) when the value of W will be at the level of ≥ 100 W $\simeq 10^{21}$ photon/sec. The phase difference between oscillations in two Fabri-Perot resonators pumped by such a laser is expected to be measured with the error of $\simeq 10^{-10}$ rad.

The scheme of laser which we analyze is presented at fig. 3: the resonator AB, containing solid state active media (shown by dashed line on the fig. 3), is coupled with reference cavity CD. We assume that:

1. All the mirrors have no losses and the mirror A is ideally reflecting one. Thus the power W is irradiated only through the mirror D.

2. The mirrors A, B and the solid state active media are rigidly assembled and the length of solid state active media are equal to the distance between mirrors A and B.

3. The finesses $\mathcal{F}$ of the mirrors B, C and D are assumed to be equal for simplicity, but the length l_{AB} of AB is much smaller than the length l_{CD} of CD. Thus the resonator AB cavity decay rate (bandwidth) γ_{AB} is much larger than the resonator CD cavity decay rate γ_{CD} ($\gamma_{AB}/\gamma_{CD} = l_{CD}/2l_{AB} \gg 1$).

4. The resonators AB and CD are optimally coupled and their mean frequencies ω_0 coincide. Therefore the output frequency mean value is very close to the CD resonance frequency and the frequency random deviations have to be substantially reduced due to the high quality $Q = \omega/(2\gamma_{CD})$ of the CD.

5. The solid state active media have negligible losses near the operating wavelength λ, and we also assume the random distortions of this solid body due to Brownian motion in itself are possible not to be taken into account.

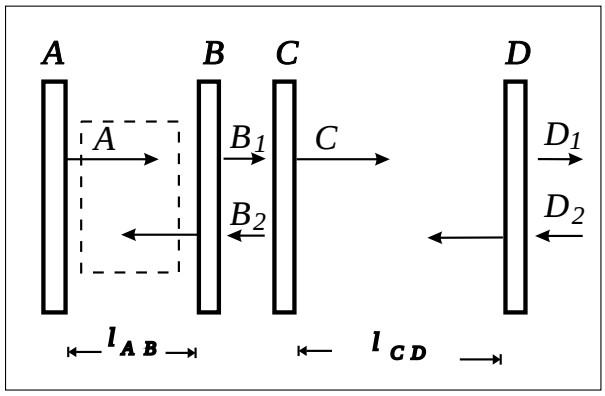

FIG. 5. The laser scheme. Resonator formed by the mirrors A and B contains the active media shown by the dashed line. The reference cavity is formed by the mirrors C and D. The mirror A is fully reflecting thus the power is irradiated only through the mirror D.

Under these assumptions we can write down the general expression for the output radiation frequency fluctuations spectral density $S_\omega(\Omega)$ for the laser working far above the threshold[2]:

[2]We use "one-sided" spectral density, defined only for positive frequencies, which may be calcu-

$$\frac{S_\omega(\Omega)}{\omega_0^2} = \frac{S_{0\omega}(\Omega)}{\omega_0^2} + \frac{S_{\Delta\omega}(\Omega)}{\omega_0^2}, \tag{70}$$

$$\frac{S_{0\omega}(\Omega)}{\omega_0^2} \simeq \frac{\hbar\omega_0}{W}\left[\left(\frac{\gamma_{CD}}{\omega_0}\right)^2 + \frac{1}{2}\left(\frac{\Omega}{\omega_0}\right)^2\right], \tag{71}$$

$$\frac{S_{\Delta\omega}(\Omega)}{\omega_0^2} = \frac{1}{\omega_0^2}\left\{\left(\frac{l_{AB}}{2l_{CD}}\right)^2 S_{\Delta\omega_{AB}} + S_{\Delta\omega_{CD}}\right\}. \tag{72}$$

See details of calculations in Appendix F2. Here Ω is the observation frequency. The first term $S_{0\omega}(\Omega)$ in (70) describes the fluctuations caused by vacuum fluctuations (penetrating through mirror D) and spontaneous emission in active media: in case $\Omega \ll \gamma_{CD}$ it is practically the Townes formula in which the cavity decay rate γ_{CD} of reference cavity plays the decisive role and in opposite case when $\Omega \gg \gamma_{CD}$ this term corresponds to the phase fluctuations $\Delta\varphi^2 \simeq 1/(4N)$ of the wave irradiated through the mirror D where $N = W\tau/(\hbar\omega_0)$ is the mean number of photons irradiated during the time τ. The second term $S_{\Delta\omega}$ describes the resonators AB and CD frequency fluctuations: $S_{\Delta\omega_{AB}}$ and $S_{\Delta\omega_{CD}}$ are spectral densities of eigen frequencies fluctuations of these resonators (the resonator AB eigen frequency fluctuations contribution is suppressed by the factor $\frac{l_{AB}}{2l_{CD}}$).

The first term ($S_{0\omega}(\Omega)$) gives the major limit which for parameters listed in Appendix F1 is of the order:

$$\frac{\sqrt{S_{0\omega}(\Omega)}}{\omega_0} \simeq 1.1 \times 10^{-21}\ \frac{1}{\sqrt{\text{Hz}}}. \tag{73}$$

In the following sections we analyze several intrinsic effects which define the value of second term ($S_{\Delta\omega}(\Omega)$).

---

lated from correlation function $\langle X(t)X(t+\tau)\rangle$ using formula

$$S_X(\Omega) = 2\int_{-\infty}^{\infty} d\tau\ \langle X(t)X(t+\tau)\rangle\ \cos(\Omega\tau).$$

Consider that the only sources of frequency fluctuations are the temperature fluctuations which together with nonzero β produce random changes of optical length in AB active media and thus produce the AB resonance frequency random changes. (In this section we assume that the positions of all the mirrors A, B, C, and D do not fluctuate.) These frequency fluctuations will be substantially reduced in accordance with formula (72) due to the assumed small ratio l_{AB}/l_{CD} value. In this section we do not consider the contribution of the temperature fluctuations through thermoexpansion (coefficient α) because these effects are relatively small due to the small values of l_{AB}/l_{CD} and α.

There are two types of temperature fluctuations in the discussed scheme. The first ones are thermodynamic (TD) fluctuations (see details in [4,5] and references therein). These ones are of pure classical origin in thermal equilibrium. The second ones are of quantum origin: the optical photons from the pumping photodiodes being absorbed in the laser solid body produces random local jumps of temperature — photo-thermal shot noise (SN).

We assume that radius r_0 of light beam in solid state active media is much smaller than cross dimensions of active media and for calculations one can expand the cross dimensions of media to infinity. Therefore we have the problem to calculate the fluctuations of temperature in cylindrical volume with radius r_0 and length l_{AB} in the infinite layer with the width l_{AB} (the cylinder axis is perpendicular to the layer). The results of calculations for photo-thermal shot noise (noted by superscript $^{\rm SN}$) and the temperature thermodynamic fluctuations (noted by superscript $^{\rm TD}$) may be presented in the following form:

$$\frac{\sqrt{S^{\rm SN}_{\Delta\omega_{AB}}(\Omega)}}{\omega_0} = \beta\sqrt{\frac{\hbar\omega_0 W}{(C\rho)^2\pi r_0^2 l_{AB}\, V\,\Omega^2}}, \tag{74}$$

$$\frac{l_{AB}}{2l_{CD}}\,\frac{\sqrt{S^{\rm SN}_{\Delta\omega_{AB}}(\Omega)}}{\omega_0} \simeq 2.2\times 10^{-21}\ \frac{1}{\sqrt{\rm Hz}},$$

$$\frac{\sqrt{S^{\rm TD}_{\Delta\omega_{AB}}(\Omega)}}{\omega_0} = \sqrt{\frac{4\kappa T^2\lambda^*}{(C\rho)^2\pi r_0^4 l_{AB}\,\Omega^2}}, \tag{75}$$

$$\frac{\beta\, l_{AB}}{l_{CD}} \frac{\sqrt{S^{\rm TD}_{\Delta\omega_{AB}}(\Omega)}}{\omega_0} \simeq 1.8 \times 10^{-20}\ \frac{1}{\sqrt{\rm Hz}}.$$

Here λ^* is thermal conductivity, ρ is density and C is specific heat capacity of active media, κ is Boltzman constant, T is absolute temperature, V is effective volume, W is absorbed power (all over below we assume power absorbed in active media is equal to optical power irradiated by laser for simplicity). Here we also use the adiabatic approximation $\Omega \gg \lambda^*/(\rho C\, r_0^2)$. For numerical estimates we used material parameters of nondoped Nd:YAG. Details of calculations are presented in Appendix F3.

We see that thermorefractive effect caused by the temperature TD fluctuations increases considerably the frequency fluctuations — its contribution is about 16 times larger than Townes limit (compare (75) and (73)).

Fluctuations of Reference Cavity

SQL of Frequency

The Standard Quantum Limit (SQL) existance for self-sustained oscillator was predicted more that 20 years ago [12]. This limit origin is very simple: the output optical radiation "brings out" the information about the coordinate (in our scheme the frequency is linearly connected with the distance between the mirrors C and D). During the continuous coordinate measurement process the momentum of the masses (in our case they are the mirrors C and D) have to be inevitably perturbed. In other words, the Heisenberg uncertainty principle has to be fulfilled. The momentum perturbation origin is well known: these are the random "kicks" of optical photons on the mirrors. This effect in essence is nonlinear because it is created by the fluctuations of the ponderomotive pressure of the optical field inside the Fabri-Perot resonator. If the mirrors C and D can be regarded as free equal masses $m_C = m_D$ (the eigen frequency of the mechanical suspension is much smaller than

the observation frequency Ω) then the frequency fluctuations SQL is equal to[3]

$$\frac{\sqrt{S^{\rm SQL}_{\Delta\omega_{CD}}(\Omega_0)}}{\omega_0} = \sqrt{\frac{8\hbar}{m_C l_{CD}^2 \Omega_0^2}} \simeq 1.4 \times 10^{-21} \frac{1}{\sqrt{\rm Hz}}, \tag{76}$$

which is achieved at the optimal output power W_{opt}:

$$W_{\rm opt} = \frac{\pi^2 m_C\, c_0^2\, \Omega_0^2}{16\, \omega_0 \mathcal{F}^2} \simeq 12 \text{ Watt}. \tag{77}$$

where c_0 is the velocity of light. These formulae are obtained in approximation $\gamma_{CD} \gg \Omega$ however for opposite case $\gamma_{CD} \ll \Omega$ it differs by factor about unity only.

It is important that frequency SQL (76) decreases when the distance l_{CD} increases, whereas optimal power W_{opt} does not depend on the length l_{CD} and depends on the mirror finesse $\mathcal{F}$.

It is worth to note that the limit (76) is valid only for specific frequency Ω_0 defining the optimal power (77). In general case for arbitrary frequency Ω and power W the frequency fluctuations are bigger:

$$\frac{\sqrt{S^{\rm PM}_{\Delta\omega_{CD}}(\Omega)}}{\omega_0} = \sqrt{\frac{4\hbar}{m_C l_{CD}^2 \Omega_0^2} \left(\frac{W_{opt}}{W} + \frac{W}{W_{opt}} \left(\frac{\Omega_0}{\Omega} \right)^4 \right)}.$$

Mirrors C and D Surface Fluctuations

Unfortunately, apart from mentioned sources of noise there are additional ones which change the effective distance l_{CD}:

1. Thermodynamic temperature fluctuations cause the mirror surface fluctuations due to nonzero thermal expansion coefficient α. These fluctuations are also called as thermoelastic noise.

---

[3]The similar AB ponderomotive pressure fluctuations are substantially smaller and were not taken into account in previous section because the mirrors A, B and active media had been assumed to be rigidly assembled, and the lowest mechanical eigen frequency of such a set is much higher than Ω. The frequency fluctuations SQL of such a set (without reference cavity) was analyzed in [12].

2. Thermal shot noise temperature fluctuations cause the mirror surface fluctuations due to nonzero thermal expansion coefficient α.

3. The noise associated with the mirrors' material is inevitably related to the mechanical losses which can be originated by different physical mechanisms. We use the model of structural damping and denote it as Brownian motion of the surface. In this model the loss angle ϕ does not depend on frequency [10].

These effects are analyzed in details in [4] and we give only final formulae denoted by superscripts $^{\rm TD}$ and $^{\rm B}$ for thermodynamic fluctuations and Brownian fluctuations correspondingly (the thermal shot noise effect is substantially smaller and we do not present formula for it):

$$\frac{S^{\rm TD}_{\Delta\omega_{CD}}(\Omega)}{\omega_0^2} = \frac{16}{\sqrt{2\pi}}\,\frac{\alpha^2\kappa T^2(1+\sigma)^2\lambda^*}{(\rho C)^2 r_0^3\Omega^2 l_{CD}^2}, \tag{78}$$

$$\text{Fused silica:}\quad \sqrt{\frac{S^{\rm TD}_{\Delta\omega_{CD}}(\Omega)}{\omega_0^2}} \simeq 6.6\times 10^{-23}\,\frac{1}{\sqrt{\rm Hz}},$$

$$\text{Sapphire:}\quad \sqrt{\frac{S^{\rm TD}_{\Delta\omega_{CD}}(\Omega)}{\omega_0^2}} \simeq 1.6\times 10^{-20}\,\frac{1}{\sqrt{\rm Hz}},$$

$$\frac{S^{\rm B}_{\Delta\omega_{CD}}(\Omega)}{\omega_0^2} \simeq \frac{8}{\sqrt{2\pi}}\,\frac{\kappa T(1-\sigma^2)}{r_0\Omega\, E\, l_{CD}^2}\,\phi, \tag{79}$$

$$\text{Fused silica:}\quad \sqrt{\frac{S^{\rm B}_{\Delta\omega_{CD}}(\Omega)}{\omega_0^2}} \simeq 5.4\times 10^{-21}\,\frac{1}{\sqrt{\rm Hz}},$$

$$\text{Sapphire:}\quad \sqrt{\frac{S^{\rm B}_{\Delta\omega_{CD}}(\Omega)}{\omega_0^2}} \simeq 5.4\times 10^{-22}\,\frac{1}{\sqrt{\rm Hz}}.$$

Here σ is the Poison ratio and E is the Young modulus. For thermodynamic fluctuations we also use adiabatic approximation $\Omega \gg \lambda^*/(\rho C\, r_0^2)$. The estimations are given for two kinds of mirror material: fused silica and sapphire. We see that these fluctuations are not small and may exceed the SQL fluctuations for chosen numerical parameters.

Thermorefractive Noise in Mirrors

Thermodynamic temperature fluctuations together with photothermal shot noise also originate the thermorefractive fluctuations: the mirror coating optical layers effective re-

fractive indexes fluctuations lead to these layers optical thickness fluctuations and hence to the phase noise in the reflected wave. The detailed calculations of these effects are given in [5] and below we write down only the final formulae for thermorefractive effect caused by thermodynamic temperature fluctuations (we do not present formula for thermorefractive shot noise because of its smaller numerical value):

$$\frac{S^{TR}_{\Delta\omega_{CD}}(\Omega)}{\omega_0^2} = \frac{2\sqrt{2}\,\beta_{eff}^2\lambda^2\kappa T^2}{\pi r_0^2 l_{CD}^2\sqrt{\Omega\rho C\lambda^*}}, \tag{80}$$

$$\beta_{\text{eff}} = \frac{n_2^2\beta_1 + n_1^2\beta_2}{4(n_1^2 - n_2^2)}, \quad \lambda = \frac{\omega_0}{2\pi\, c_0}. \tag{81}$$

Here β_1 and β_2 are thermorefractive coefficients for layers with refractive indexes n_1 and n_2 correspondingly. For often used pairs of layers TiO_2 - SiO_2 and Ta_2O_5 - SiO_2 we obtain the following estimates:

$$\frac{\sqrt{S^{TR}_{\Delta\omega_{CD}}(\Omega)}}{\omega_0} \simeq 1.4\times 10^{-23}\ \frac{1}{\sqrt{\text{Hz}}}, \quad (TiO_2 - SiO_2),$$

$$\frac{\sqrt{S^{TR}_{\Delta\omega_{CD}}(\Omega)}}{\omega_0} \simeq 2.5\times 10^{-23}\ \frac{1}{\sqrt{\text{Hz}}}, \quad (Ta_2O_5 - SiO_2)$$

This effect seems to be small enough for presented parameters however it has weak dependence $\sqrt{S^{TR}_{\Delta\omega_{CD}}(\Omega)} \sim 1/\sqrt[4]{\Omega}$ on observation frequency Ω and can be significant for the frequencies above 1 kHz.

Conclusion

We see that for used parameters thertmorefractive fluctuations in laser resonator makes the largest contribution into frequency instability.

The frequency instability caused by the effects considered in this article is inversely proportional to distance l_{CD} and therefore their negative influence can be suppressed by increasing the length of the reference cavity.

The effects analyzed in this article can be analytically calculated. However, there are a lot of other processes responsible for additional frequency instability, which may provide

substantial contribution especially within the band of observation frequency near 100 Hz. They are usually called as "$1/f$" noise or excess noise. For example, as "the candidate" responsible for such process, we may point to the random jumps of vacancies or the birth of dislocations in the solid objects. Unfortunately, there are no reliable theoretical model for such processes which would allow to obtain analytical formulae and numerical estimates. Thus the presented in this paper analysis may offer to experimentalists only the lower limits of the frequency instability. For real experiments this value has to be larger.

In the same time none of the noise sources analyzed in this article may be called as the fundamental one. This statement is also correct for the frequency SQL: the ponderomotive nonlinearity (which is equivalent to positive cubic nonlinearity of optical material) was emphasized in [13] and in principle can be compensated by a nonlinearity with opposite sign in solid. In this case the output radiation will "bring out" information not only about the coordinate, and the frequency deviation may be smaller. However, this potential possibility has not been seriously investigated yet.

We also think that the analysis presented above may be useful for the final choice of the optimal LIGO topology. In the ideal case when both arms of the LIGO interferometer are identical the laser frequency fluctuations are completely subtracted in output signal. For real case the symmetry level of two interferometer arms may play an important role. The requirements for symmetry level became more tough when the power recycling is used as it was planned in the LIGO-II and the LIGO-III.

Appendix F1. Parameters

For estimates we used the following parameters:

$$\omega_0 = 2 \times 10^{15}\ \mathrm{s}^{-1},\ W = 10\ \mathrm{W},$$

$$T = 300\ \mathrm{K}^\circ, \quad m_c = 10\ \mathrm{kg},$$

$$\Omega = 2\pi \times 100\ \mathrm{s}^{-1}, \quad r_0 = 0.5\ \mathrm{cm}$$

$l_{AB} = 30$ cm, $\quad l_{CD} = 10^3$ cm,

$V = 2 \times (\pi r_0^2 l_{AB}) \simeq 50$ cm^3,

$\mathcal{F} = 3 \times 10^3, \quad \gamma_{CD} = \dfrac{\pi c}{2\mathcal{F} l_{CD}} \simeq 1.5 \times 10^4$ s^{-1},

Nd:YAG:

$C = 1.4 \times 10^7$ erg/(g K°), $\quad \rho = 4.55$ g/cm^3,

$\lambda^* = 1.4 \times 10^6$ erg cm/(s K°),

$\beta = 0.7 \times 10^{-5}$ (K°)$^{-1}$,

Fused silica:

$C = 6.7 \times 10^7$ erg/(g K°), $\quad \rho = 2.2$ g/cm^3,

$\lambda^* = 1.4 \times 10^5$ erg cm/(s K°),

$E = 7.2 \times 10^{11}$erg/cm^3, $\quad \sigma = 0.17$,

$\phi = 5 \times 10^{-8}, \quad \alpha = 5.5 \times 10^{-7}$ (K°)$^{-1}$,

Sapphire:

$C = 7.9 \times 10^6$ erg/(g K°), $\quad \rho = 4.0$ g/cm^3,

$\lambda^* = 4.0 \times 10^6$ erg cm/(s K°),

$E = 4 \times 10^{12}$ erg/cm^3, $\quad \sigma = 0.29$,

$\alpha = 5.0 \times 10^{-6}$ (K°)$^{-1}$, $\quad \phi = 3 \times 10^{-9}$.

The material parameters (C, ρ, λ^*, α, β) are given for fused silica, sapphire [4], and nondoped YAG [11].

For estimates of the thermorefractive effect we used the following optical parameters for the mirror coatings layers:

$$n_1 = 2.2, \qquad \beta_1 = 4 \cdot 10^{-5} \text{ K}^{-1} \quad (Ti O_2),$$

$$n_1 = 2.2, \qquad \beta_1 = 6 \cdot 10^{-5} \text{ K}^{-1} \quad (Ta_2 O_5),$$

$$n_2 = 1.45, \qquad \beta_2 = 1.5 \cdot 10^{-5} \text{ K}^{-1} \quad (Si O_2).$$

Appendix F2. Fluctuations of frequency

In this Appendix we present the calculations of general formula (70) for frequency fluctuations.

Below we use the complex amplitudes ($A,\ B\ C\ D$ shown on figure 5) related to the electric field E and the mean power W by the following equations

$$E = A(t)\sqrt{\frac{\hbar\omega_0}{Sc_0}}e^{-i\omega_0 t} + \text{h.c.}, \quad W = \frac{Sc_0\langle E^2\rangle}{4\pi} = \frac{\hbar\omega_0 A^2}{2\pi},$$

where S is the cross-section of the light beam, c_0 is the velocity of light. Complex amplitude (for example $A(t)$) is written below as a sum of the constant mean amplitude (denoted by capital letter with zero superscript) and the fluctuation part (denoted by small letter):

$$\begin{aligned} A(t) &= e^{-i\omega_0 t}(A^0 + a(t)) + \text{h.c.}, \\ a(t) &= \int_{-\infty}^{\infty} \sqrt{1+\frac{\Omega}{\omega_0}}\, a(\Omega)\, e^{-i\Omega t}\, d\Omega, \qquad (82) \\ [a(\Omega), a(\Omega')] &= 0, \quad \left[a(\Omega), a^+(\Omega')\right] = \delta(\Omega - \Omega'), \\ \left[a(t), a^+(t')\right] &= 2\pi\delta(t-t'). \qquad (83) \end{aligned}$$

We assume below that $\Omega \ll \omega_0$ and drop the term $\sqrt{1+\frac{\Omega}{\omega_0}}$ under the integral in (82).

We write down the equation for the complex amplitude A describing the field within the resonator AB:

$$\dot{A} + (\gamma - \delta + k|A|^2)\, A = \sqrt{\frac{c_0\gamma_{AB}}{l_{AB}}}(B_2 + e_{\text{sp}}), \qquad (84)$$
$$+iA\,\Delta\omega_{AB}.$$

Here δ and k are the constants describing negative nonlinear losses, e_{sp} is the additional noise caused by spontaneous emission in the active media. The last term describes the fluctuations of the resonator frequency. For the complex amplitude C (in the resonator CD) we have the following equation:

$$\dot{C} + \gamma_{CD}\, C = \sqrt{\frac{c_0\gamma_{CD}}{2l_{CD}}}\,(D_2 + B_1) + iB_3\Delta\omega_{CD}. \qquad (85)$$

These equations have to be supplemented by the boundary conditions on the mirrors B, C and D:

$$B_1 = -B_2\sqrt{1-T} + A\sqrt{T},$$
$$B_2 = -C\sqrt{T} - B_1\sqrt{1-T},$$
$$D_1 = -D_2\sqrt{1-T} + C\sqrt{T}.$$

Here T is the transparency coefficient (remind that the mirrors B, C and D have the same transparency).

Now we consider every amplitude as a sum of the mean constant value and the small fluctuation part. For the mean amplitudes we have:

$$A^0 = C^0 = \sqrt{\frac{\delta-\gamma}{k}}, \quad D_1^0 = B_1^0 = A^0\sqrt{T}, \quad B_2^0 = 0.$$

For the fluctuation components we use linear approximation keeping the terms $\sim \sqrt{T}$ and assuming $\sqrt{1-T} \simeq 1$:

$$\partial_t a + (\delta-\gamma)(a+a^+) = \sqrt{\frac{c_0\gamma_{AB}}{l_{AB}}}(b_2 + e_{\rm sp}) + iA^0\Delta\omega_{AB},$$
$$\dot{c} + \gamma_{CD}\, c = \sqrt{\frac{c_0\gamma_{CD}}{2l_{CD}}}(d_2 + b_1) + iC^0\Delta\omega_{mc},$$
$$b_1 = -b_2 - a\sqrt{T}, \quad b_2 = c\sqrt{T} - b_1, \quad d_1 = -d_2 + c\sqrt{T}.$$

Fourier transform of the output radiation phase component $\mathcal{D}_1^{\rm ph}(\Omega)$ may be obtained after long but simple calculations:

$$\begin{aligned}\mathcal{D}_1^{ph}(\Omega) = {} & \frac{\Omega^2(\gamma_{CD}+2\gamma_{AB}) + \gamma_{CD}^2(2\gamma_{AB}+i\Omega)}{(\gamma_{CD}-i\Omega)(\gamma_{CD}+2\gamma_{AB})}\,\frac{\mathcal{D}_2^{ph}(\Omega)}{(-i\Omega)} + \\ & + \frac{2\gamma_{AB}\gamma_{CD}}{-i\Omega(\gamma_{CD}+2\gamma_{AB})}\,\mathcal{E}_{\rm sp}^{ph}(\Omega) + \\ & + \frac{D_1^0}{(-i\Omega)}\left(\frac{\Delta\omega_{AB}\,\gamma_{CD}}{(\gamma_{CD}+2\gamma_{AB})} + \frac{2\Delta\omega_{CD}\,\gamma_{AB}}{(\gamma_{CD}+2\gamma_{AB})}\right), \\ \mathcal{D}_1^{ph} = {} & \frac{d_1+d_1^+}{2i}, \quad \mathcal{D}_2^{ph} = \frac{d_2+d_2^+}{2i}, \quad \mathcal{E}_{\rm sp}^{ph} = \frac{e_{\rm sp}+e_{\rm sp}^+}{2i}.\end{aligned} \tag{86}$$

Assuming that $\gamma_{AB} \gg \gamma_{CD}$ the expression for $\mathcal{D}_1^{ph}(\Omega)$ can be simplified resulting in:

$$\mathcal{D}_1^{ph}(\Omega) \simeq \frac{i(\gamma_{CD} - i\Omega)}{\Omega}\mathcal{D}_2^{ph}(\Omega) + \frac{\gamma_{CD}}{-i\Omega}\,\mathcal{E}_{\rm sp}^{ph}(\Omega) + \\ + \frac{D_1^0}{(-i\Omega)}\left(\Delta\omega_{AB}\,\frac{\gamma_{CD}}{2\gamma_{AB}} + \Delta\omega_{CD}\right)$$

Assume the spectral density $S_{D2}^{ph}(\Omega)$ of $\mathcal{D}_2^{ph}$ fluctuations corresponds to the vacuum fluctuations and is equal to the spectral density $S_{Esp}^{ph}(\Omega)$ of spontaneous noise $\mathcal{E}_{\rm sp}^{ph}$:

$$\langle \mathcal{D}_2^{ph}(t)\mathcal{D}_2^{ph}(t')\rangle = \frac{2\pi}{4}\,\delta(t-t'),$$
$$S_{D2}^{ph}(\Omega) = 2\int_{-\infty}^{\infty} dt\; e^{-i\Omega t}\langle \mathcal{C}_3^{ph}(0)\mathcal{C}_3^{ph}(t)\rangle = \pi,$$
$$S_{Esp}^{ph}(\Omega) = S_{D2}^{ph}(\Omega) = \pi.$$

Then the output radiation phase fluctuations spectral density can be obtained as follows:

$$S_\varphi(\Omega) = \frac{S_{D2}^{ph}(\Omega)}{|D^0|^2} = \frac{h\omega_0}{2W}\left(2\left(\frac{\gamma_{CD}}{\Omega}\right)^2 + 1\right) + \\ + \frac{\left(\frac{\gamma_{CD}}{2\gamma_{AB}}\right)^2 S_{\Delta\omega_{AB}} + S_{\Delta\omega_{CD}}}{\Omega^2}. \qquad (87)$$

Using (87) the formula (70) can be easy obtained.

Appendix F3. Thermorefractive fluctuations in infinite layer

In this Appendix we present calculations for the laser resonator AB thermorefractive fluctuations formulae (74, 75.

Thermal Shot Noise

For calculation of temperature u fluctuations in infinite layer with thermoisolated boundary that caused by shot noise fluctuations, we have the equation of thermal conductivity (for this case z-axis is perpendicular to the layer):

$$C\rho\partial_t u - \lambda^*\Delta u = w(\vec{r},t), \qquad (88)$$

$$\partial_z u\big|_{z=0} = 0, \qquad \partial_z u\big|_{z=h} = 0, \qquad (89)$$

$$\langle w(\vec{r},t)w(\vec{r}',t')\rangle = \hbar\omega_0\, W_0\,\delta(t-t')\,\delta(\vec{r}-\vec{r}').$$

Here W_0 is averaged power absorbed in a unit volume. We assume that $W_0 = W/V$ where W is the total averaged power absorbed in whole volume V of the laser active media. We write the solution as a Fourier-series expansion

$$u(t,\vec{r}_\perp,z) = \int_{-\infty}^{\infty} \frac{dk_x dk_y d\omega}{(2\pi)^3} \sum_{n=0}^{\infty} \cos(b_n z) \times$$
$$\times e^{i\omega t - ik_x x - ik_y y} \frac{w_n(\omega,\vec{k}_\perp)}{C\rho(a^2k^2 + i\omega)},$$
$$b_n = \frac{\pi n}{l_{AB}}, \quad a^2 = \frac{\lambda^*}{C\rho},$$
$$\vec{r}_\perp = \vec{e}_x x + \vec{e}_y y, \quad \vec{k}_\perp = \vec{e}_x k_x + \vec{e}_y k_y,$$
$$\langle w_n(\omega,\vec{k}_\perp) w_{n'}(\omega',\vec{k}'_\perp)\rangle = \hbar\omega_0 W_0 \times$$
$$\times 2\pi\,\delta(\omega-\omega') \times \frac{2-\delta_{0\,n}}{l_{AB}}\,\delta_{n\,n'} \times (2\pi)^2\,\delta(\vec{k}_\perp - \vec{k}'_\perp).$$

We are interested in the fluctuations of temperature $\bar{u}$ averaged over the beam volume:

$$\bar{u}(t) = \int_0^{l_{AB}} \frac{dz}{l_{AB}} \int_{-\infty}^{\infty} \frac{dx\,dy}{\pi r_0^2}\; e^{-(x^2+y^2)/r_0^2}\; u(t,\vec{r}),$$
$$\bar{u}(\omega) = \int_{-\infty}^{\infty} \frac{dk_x dk_y}{(2\pi)^2}\, e^{-(k_y^2+k_z^2)r_0^2/4} \times$$
$$\times \frac{w_0(\omega,\vec{k}_\perp)}{C\rho(a^2k_\perp^2 + i\omega)},$$
$$\langle \bar{u}(\omega)\bar{u}(\omega')\rangle = 2\pi\,\delta(\omega-\omega') \times \frac{\hbar\omega_0 W_0}{(C\rho)^2 l_{AB}} \times$$
$$\times \int_{-\infty}^{\infty} \frac{dk_x dk_y}{(2\pi)^2} \times \frac{e^{-k_\perp^2 r_0^2/2}}{a^4k_\perp^4 + \omega^2}.$$

Using adiabatic approximation $\omega \gg a^2/r_0^2$ the term $\sim a^4k^4$ in the last fraction denominator can be dropped. Then the expression for spectral density $S_{\bar{u}}^{\rm TS}(\omega)$ of averaged temperature $\bar{u}$ will be the following:

$$S_{\bar{u}}^{\rm TS}(\omega) \simeq \frac{2\hbar\omega_0 W_0}{(C\rho\, l_{AB})^2\omega^2} \times \int_{-\infty}^{\infty} \frac{dk_x dk_y}{(2\pi)^2}\, e^{-k_\perp^2 r_0^2/2} =$$
$$= \frac{\hbar\omega_0 W}{(C\rho)^2\pi r_0^2 l_{AB}\, V\, \omega^2} \qquad (90)$$

The formula (74) can be easily obtained from (90).

TD Temperature Fluctuations

For the TD temperature u fluctuations calculation in infinite layer we use the Langevin approach, i. e. we add fluctuation forces into the thermal conductivity equation right side (see details in [4]):

$$C\rho\partial_t u - \lambda^*\Delta u = F(\vec{r},t), \tag{91}$$

$$\partial_z u|_{z=0} = 0, \quad \partial_z u|_{z=l_{AB}} = 0 : \tag{92}$$

$$\langle F(\vec{r},t)F(\vec{r}',t')\rangle = -2\kappa T^2\lambda^*\,\delta(t-t')\,\Delta\delta(\vec{r}-\vec{r}').$$

We write the solution as a Fourier-series expansion

$$u(t,\vec{r}_\perp,z) = \int_{-\infty}^{\infty}\frac{dk_x dk_y d\omega}{(2\pi)^3}\sum_{n=0}^{\infty}\cos(b_n z)\times \tag{93}$$

$$\times e^{i\omega t - ik_x x - ik_y y}\,\frac{F_n(\omega,\vec{k}_\perp)}{C\rho(a^2k^2+i\omega)},$$

$$b_n = \frac{\pi n}{l_{AB}}, \quad a^2 = \frac{\lambda^*}{C\rho},$$

$$\vec{r}_\perp = \vec{e}_x x + \vec{e}_y y, \quad \vec{k}_\perp = \vec{e}_x k_x + \vec{e}_y k_y,$$

$$\langle F_n(\omega,\vec{k}_\perp)F_{n'}(\omega',\vec{k}'_\perp)\rangle =$$

$$= 2\kappa T^2\lambda^* 2\pi\,\delta(\omega-\omega')\times\frac{2-\delta_{0\,n}}{l_{AB}}\,\delta_{n\,n'}\times$$

$$\times(2\pi)^2\,\delta(\vec{k}_\perp - \vec{k}'_\perp)\times(b_n^2+k_\perp^2). \tag{94}$$

We are interested in fluctuations of temperature $\bar{u}$ averaged over the beam volume:

$$\bar{u}(t) = \int_{-l_{AB}/2}^{l_{AB}/2}\frac{dz}{l_{AB}}\int_{-\infty}^{\infty}\frac{dx\,dy}{\pi r_0^2}\;e^{-(x^2+y^2)/r_0^2}\;u(t,\vec{r}),$$

$$\bar{u}(\omega) = \int_{-\infty}^{\infty}\frac{dk_x dk_y}{(2\pi)^2}\times$$

$$\times e^{-(k_y^2+k_z^2)r_0^2/4}\,\frac{F_0(\omega,\vec{k}_\perp)}{C\rho(a^2k_\perp^2+i\omega)},$$

$$\langle\bar{u}(\omega)\bar{u}(\omega')\rangle = 2\pi\,\delta(\omega-\omega')\times\frac{2\kappa T^2\lambda^*}{(C\rho)^2 l_{AB}}\times$$

$$\times\int_{-\infty}^{\infty}\frac{dk_x dk_y}{(2\pi)^2}\times\frac{k_\perp^2\,e^{-k_\perp^2 r_0^2/2}}{a^4k_\perp^4+\omega^2}.$$

Using adiabatic approximation $\omega \gg a^2/r_0^2$ the term $\sim a^4k^4$ in the last fraction denominator can be dropped. Then the expression for spectral density $S_{\bar{u}}^{\rm TD}(\omega)$ of averaged temperature $\bar{u}$ will be the following:

$$S_{\bar{u}}^{\mathrm{TD}}(\omega) \simeq \frac{4\kappa T^2 \lambda^*}{(C\rho)^2 l_{AB}} \int_{-\infty}^{\infty} \frac{k_\perp \, dk_\perp}{2\pi} \, e^{-k_\perp^2 r_0^2/2} \, \frac{k_\perp^2}{\omega^2} = \tag{95}$$

$$= \frac{4\kappa T^2 \lambda^*}{(C\rho)^2 \pi r_0^4 l_{AB} \, \omega^2}. \tag{96}$$

The formula (75) can be easily obtained from (96).

REFERENCES

[1] A. Abramovici *et al.*, *Science* **256** (1992) 325.

[2] A. Abramovici *et al.*, *Physics Letters A* **218** (1996) 157.

[3] G. Rempe, R. Thompson, Y. J. Kimble, *Optics Letters*, **17** (1992) 362

[4] V. B. Braginsky, M. L. Gorodetsky, and S. P. Vyatchanin, *Physics Letters* **A 264** (1999) 1 ; cond-mat/9912139.

[5] V. B. Braginsky, M. L. Gorodetsky, and S. P. Vyatchanin, *Physics Letters* **A 271** (2000) 303.

[6] Yu. T. Liu and K. S. Thorne, submitted to *Phys. Rev. D.*

[7] B. Zhou, T. J. Kane, G. J. Dixon and R. L. Byer, *Optics Letters* **10** (1985) 62.

[8] T. J. Kane and R. L. Byer, *Optics Letters* **10** (1985) 65.

[9] W. Wiechnann, T. J. Kane, D. Haserot, F. Adams, G. Tuong, J. D. Kmetec, *Proceedings of CLEO'98* (1998) 432.

[10] P. R. Saulson, *Rhys. Rev. D*, **42** (1990) 2437;
G. I. Gonzalez and P. R. Saulson, *J. Acoust. Soc. Am.*, **96** (1994) 207.

[11] F.Bondu, *Report on Aspen Winter Conference on Gravitational Waves and their Detection*, Feb 20-26, 2000.

[12] V. B. Braginsky and S. P. Vyatchanin, *Zh. Eksp. i Teor. Fiz.*, **74** (1978) 828,
English translation: *Sov. Phys. JETP*, **47** (1978) 433.

[13] V. B. Braginsky, V. I. Panov and S. P. Vyatchanin, *Doklady AN SSSR*, **247** (1979) 583
English translation: *Physics-Doklady*, **24** (1979) No. 7.

Appendix G. The Discrete Sampling Variation Measurement

Introduction

It is common knowledge that the sensitivity of traditionally designed position meters, including interferometric meters used in the large-scale gravitational wave detectors, is limited by the Standard Quantum Limit (SQL) [1]. One of the most promising ways of evading the SQL is the variation quantum measurement [2] because it requires minimal modifications in the interferometric meters hardware setup only. This method makes it possible to eliminate the output signal fluctuations caused by the back action of the meter simply by proper modulation of the local oscillator phase $\phi_{\rm LO}$.

Unfortunately the function $\phi_{\rm LO}(t)$ used in the variation measurement depends on the signal shape and arrival time. This dependance of the meter hardware setup on the signal shape is the main disadvantage of the variation measurement. Because of this disadvantage the variation measurement in its original version can be used for detection of determenistic signals only.

In the article [2] the modified version of the above mentioned procedure had been proposed and considered in brief. It allows to circumvent this disadvantage and makes it possible to monitor the signal shape. This method is based on the signal approximation by series of short rectangular "slices" and periodical applying the variation measurement procedure fitted to such a rectangular pulse. We propose to name this procedure "discrete sampling variation measurement"(DSVM). In this paper we consider this method in details, applying to the cases of free mass and harmonic oscillator.

In the next section we review briefly the variation measurement as it was proposed in the original works [4,3] and introduce some useful notations. In the section II we describe the discrete sampling variation measurement and in the section II we compare its sensitivity with the Standard Quantum Limit and the Energetic Quantum Limit.

Any position meter can be reduced to the simple abstract scheme presented on Fig.6. Its output signal $\tilde{x}(t)$ can be written as a sum

$$\tilde{x}(t) = x(t) + x_{\rm fluct}(t)\,, \tag{97}$$

where $x(t)$ is the test body "real" position and $x_{\rm fluct}(t)$ is noise added by the meter. On the other hand due to the uncertainty relation the meter perturbs the test body motion by the random back action force $F_{\rm fluct}(t)$. Hence the value of $x(t)$ presents a sum of three components: the test object unperturbed motion $x_{\rm init}$, response on external classical force $F_{\rm signal}$ which should be detected and response on back action force:

$$x(t) = x_{\rm init}(t) + \mathbf{D}^{-1}[F_{\rm signal}(t) + F_{\rm fluct}(t)]\,, \tag{98}$$

where $\mathbf{D}$ is the linear differential operator describing the dynamics of the test object. To take an example, for an oscillator with mass m and eigenfrequency ω_m.

$$\mathbf{D} = m\frac{d^2}{dt^2} + m\omega_m^2 \tag{99}$$

In the case of the interferometric meters $F_{\rm fluct}(t)$ is produced by the optical pumping power shot noise. The noise $x_{\rm fluct}(t)$ is the mix of the output optical beam amplitude and phase fluctuations with the weights depending on the local oscillator phase $\phi_{\rm LO}$.

In this article we will limit ourselves for simplicity by the case when both of these noises can be considered as white ones. This condition becomes invalid only for very long interferometers using the signal-recycling technique. It can be shown that the main results of our consideration are held true in this case too.

In the case of the interferometric meter with the resonant pumping spectral densities of the noises $x_{\rm fluct}(t)$ and $F_{\rm fluct}(t)$, and its cross spectral density are equal to

$$\begin{aligned} S_x &= \tfrac{\hbar L^2}{16Q\mathcal{E}\sin^2\phi_{\rm LO}} \\ S_F &= \tfrac{4\hbar Q\mathcal{E}}{L^2}\,, \\ S_{xF} &= -\tfrac{\hbar}{2}\cot\phi_{\rm LO}\,, \end{aligned} \tag{100}$$

where L is the interferometer arm length, $\mathcal{E}$ is the energy stored in it, Q is the optical resonator quality factor. It is easily to see that they satisfy the uncertainty relation

$$S_x S_F - S_{xF}^2 = \frac{\hbar^2}{4} \tag{101}$$

which is a general property of any position meter [see [5]].

It is convenient to rewrite the noise $x_{\rm fluct}$ as

$$x_{\rm fluct} = x_{\rm fluct}^{(0)} + a F_{\rm fluct}\,, \tag{102}$$

where

$$a = \frac{S_{xF}}{S_F}\,, \tag{103}$$

and $x_{\rm fluct}^{(0)}$ is the part of $x_{\rm fluct}$ uncorrelated with the back action noise. In the case of the interferometric meter this noise is produced by the output beam phase fluctuations. In this case its spectral density is equal to

$$S_x^{(0)} = \frac{\hbar^2}{4S_F} = \frac{\hbar L^2}{16 Q \mathcal{E}}\,, \tag{104}$$

and

$$a = -\frac{L^2}{8Q\mathcal{E}} \cot\phi_{\rm LO}\,. \tag{105}$$

It is important to note that a depends on time if $\phi_{\rm LO}$ is time-dependant.

The output signal $\tilde{x}(t)$ should be processed in order to optimally extract information about $F_{\rm signal}$. This signal processing can be represented as a two-stage process. At the first stage the operator $\mathbf{D}$ is applied to $\tilde{x}(t)$ in order to eliminate term $x_{\rm init}$:

$$\tilde{F}(t) = \mathbf{D}\tilde{x}(t) = F_{\rm signal}(t) + F_{\rm noise}(t)\,, \tag{106}$$

where

$$F_{\rm noise}(t) = F_{\rm fluct}(t) + \mathbf{D} x_{\rm fluct}(t)\,, \tag{107}$$

is the total noise. At the second stage $\tilde{F}(t)$ is integrated with optimally chosen filter function $v(t)$ which gives the signal required parameter estimation of the required parameter, for example, for the force amplitude A:

$$\tilde{A} = \int_{-\infty}^{\infty} v(t)\tilde{F}(t)\,dt = \int_{-\infty}^{\infty} v(t)[F_{\rm signal}(t) + F_{\rm fluct}(t) + \mathbf{D}x^{(0)}_{\rm fluct}(t) + \mathbf{D}a(t)F_{\rm fluct}(t)]\,dt\,. \quad (108)$$

It is easy to show that if $a(t)$ satisfies the equation

$$a(t)\mathbf{D}v(t) + v(t) = 0 \quad (109)$$

then two terms in (108) containing the back action force $F_{\rm fluct}(t)$ are compensate each other.[4] Hence the measurement precision in this case is limited by the noise $x^{(0)}_{\rm fluct}$ only:

$$(\Delta A)^2 = S_x^{(0)} \int_{-\infty}^{\infty} [\mathbf{D}v(t)]^2\,dt\,. \quad (110)$$

This is the basic principle of the variation measurement which permits in concept to obtain any necessary sensitivity by reducing the value of $S_x^{(0)}$.

The discrete sampling variation measurement

Suppose that *a priori* information is available for the experimentalist that the signal spectrum is limited by some value of ω_{max}. In this case small "slice" of the signal with duration $\tau \lesssim \omega_{max}^{-1}$ can be approximated by rectangular pulse with the same duration. This allows to use variation measurement with the function $a(t)$ fitted to this rectangular pulse and measure the mean value of the signal over this interval. Repeating this procedure periodically it is possible to reconstruct "slice" by "slice" the signal shape. The precision of such procedure is not limited by the SQL due to using variation measurement. On the other hand, the hardware setup here does not depend on the signal shape. The law for $\phi_{LO}(t)$

[4]Strictly speaking this is valid only if the operator $\mathbf{D}$ is "hermitian", i.e there is no dissipation in the probe object. We shall consider here this case only.

can be obtained simply by periodical repetition of a function corresponding to rectangular signal pulse.

So consider the $F_{signal}(t)$ force mean value, F_0, measurement over short time interval $-\tau/2 \le t \le \tau/2$. We suppose the test object to be a harmonic oscillator, so the operator $\mathbf{D}$ is equal to (99). Particular case of a free mass can be easily obtained by putting $\omega_m = 0$.

If the variation technique is used and back action noise is compensated then the measurement error is equal to

$$(\Delta F)^2 = S_x^{(0)} \int_{-\tau/2}^{\tau/2} [\mathbf{D}v(t)]^2 \, dt \, . \tag{111}$$

It can be shown that optimal filter function $v(t)$ must satisfy the following equation

$$\mathbf{D}^2 v(t) = \text{const} \tag{112}$$

with the normalization condition

$$\int_{-\tau/2}^{\tau/2} v(t) \, dt = 1 \tag{113}$$

and the boundary conditions

$$v(t)\Big|_{t=\pm\tau/2} = 0 \, , \quad \frac{dv(t)}{dt}\Big|_{t=\pm\tau/2} = 0 \, . \tag{114}$$

The solution is equal to

$$v(t) = \omega_m \frac{\omega_m\tau + \sin\omega_m\tau - 2\left(\sin\frac{\omega_m\tau}{2} + \frac{\omega_m\tau}{2}\cos\frac{\omega_m\tau}{2}\right)\cos\omega_m t - 2\sin\frac{\omega_m\tau}{2}\,\omega_m t\sin\omega_m t}{\omega_m\tau(\omega_m\tau + \sin\omega_m\tau) - 4(1-\cos\omega_m\tau)} \, , \tag{115}$$

and the corresponding function $a(t)$ is equal to

$$a(t) = -\frac{1}{m\omega_m^2} \cdot \frac{\omega_m\tau + \sin\omega_m\tau - 4\sin\frac{\omega_m\tau}{2}\cos\omega_m t}{\omega_m\tau + \sin\omega_m\tau - 2\left(\sin\frac{\omega_m\tau}{2} + \frac{\omega_m\tau}{2}\cos\frac{\omega_m\tau}{2}\right)\cos\omega_m t - 2\sin\frac{\omega_m\tau}{2}\,\omega_m t\sin\omega_m t} . \tag{116}$$

Substitution of this function $v(t)$ into formula (111) gives the the measurement error value:

$$(\Delta F)^2 = \frac{180 m^2\hbar^2}{S_F\tau^5} \cdot k(\omega_m\tau) \, , \tag{117}$$

where

$$k(x) = \frac{x^5(x + \sin x)}{720[x(x + \sin x) - 4(1 - \cos x)]} \,. \tag{118}$$

This function is plotted on Fig.7.

In the particular case of a free mass ($\omega_m = 0$)

$$v(t) = \frac{30(t^2 - \tau^2/4)^2}{\tau^5} \,, \tag{119}$$

$$a(t) = -\frac{1}{2m} \cdot \frac{(t^2 - \tau^2/4)^2}{6t^2 - \tau^2/2} \,, \tag{120}$$

and

$$(\Delta F)^2 = \frac{180 m^2 \hbar^2}{S_F \tau^5} \,. \tag{121}$$

It should be noted that singularities in the function $a(t)$ do not prevent realization of the described procedure. They correspond simply to values of $\phi_{\rm LO}$ equal to 0 [see equation (105)].

The graphics of the functions $v(t)$ and $\phi_{LO}(t)$ for the free mass are presented at Fig.8 and Fig.9. The corresponding graphics for the oscillator are almost the same if the parameter ω_m is chosen in the optimal way,

$$\omega_m \approx \frac{\pi}{\tau} \,. \tag{122}$$

Every repetition of this procedure on time intervals $\tau/2 \le t \le 3\tau/2$, $3\tau/2 \le t \le 5\tau/2$ and so on gives an estimation for the signal force mean value over the corresponding interval $F_{j\,\rm signal}$:

$$\tilde{F}_j = F_j + F_{j\,\rm noise} \,, \tag{123}$$

where $j = 0, 1, 2 \ldots$,

$$F_j = \int_{-\tau/2}^{\tau/2} v(t) F_{\rm signal}(t - j\tau)\, dt \,, \tag{124}$$

and $F_{j\,\rm noise}$ are the uncorrelated random values with the variance (111). The values (123) form vector $\{\tilde{F}_j\}$ that approximate the signal force.

Comparison with the SQL and the EQL

In this section we will limit ourselves by the case of a free mass only because the gain in the sensitivity which can be obtained by using an oscillator is not very significant (see Fig.7).

In order to compare proposed procedure with traditional meters we should return back to continuous representation. We have assumed F_{signal} to vary slowly during the time τ. This allows to approximate the vector $\{\tilde{F}_j\}$ by the continuous function

$$\tilde{F}(t) = F_{\rm signal}(t) + F_{\rm DSVM}(t)\,, \tag{125}$$

where $F_{\rm DSVM}(t)$ presents a noise produced by the measurement errors $F_{j\,\rm noise}$. Its spectral density is equal to

$$S_{\rm DSVM} = \tau(\Delta F)^2 = \frac{180m^2\hbar^2}{S_F\tau^4} \tag{126}$$

The Standard Quantum Limit usually defined as the ultimate sensitivity of the ordinary position meter, i.e position meter with white and non-correlated noises $x_{\rm fluct}$ and F_{fluct}. For such a meter the spectral density of the total noise is equal to

$$S_{\rm SQL}(\Omega) = S_F + \frac{\hbar^2 m^2\Omega^4}{4S_F}\,. \tag{127}$$

Minimum of this expression for any given observation frequency Ω is achieved if

$$S_F = S_F^{SQL} \equiv \frac{\hbar m\Omega^2}{2} \tag{128}$$

and is equal to

$$S_{SQL} = \hbar m\Omega^2\,. \tag{129}$$

The ratio of the spectral densities (126) and (129) is equal to

$$\xi^2_{DSVM} \equiv \frac{S_{\rm DSVM}}{S_{\rm SQL}} = \frac{180m\hbar}{S_F\Omega^2\tau^4} = \frac{360}{(\Omega\tau)^4}\cdot\frac{S_F^{SQL}}{S_F}\,. \tag{130}$$

The value of S_F for the parametric position meters (including interferometric ones) is proportional to the energy stored in them [see (100)]. Hence the last formula may be presented as

$$\xi^2_{DSVM} = \frac{360}{(\Omega\tau)^4} \cdot \frac{\mathcal{E}_{SQL}}{\mathcal{E}}\,, \tag{131}$$

where $\mathcal{E}_{SQL}$ is the energy which is necessary to achieve the level of the SQL and $\mathcal{E}$ is the energy actual value.

As it is known from the digital signal processing theory, a signal can be restored correctly if the sampling frequency is at least two times larger than the signal bandwidth. In accordance with this principle we suppose that

$$\tau = \frac{\pi}{\Omega_{\max}}\,. \tag{132}$$

In this case

$$\xi^2_{DSVM} = \frac{360}{\pi^4} \cdot \frac{\mathcal{E}_{\rm SQL}}{\mathcal{E}} \approx 3.7\ \frac{\mathcal{E}_{\rm SQL}}{\mathcal{E}}\,. \tag{133}$$

Conclusion

Precision of the proposed method is defined by the sampling period τ. The less is this value, the better temporal resolution can be obtained. On the other hand, the pumping energy required to obtain given level of sensitivity rises as τ^{-4} with reducing τ. Nevertheless if the value of τ is chosen wisely then a good balance can be achieved.

It is useful to compare the sensitivity of the proposed method (133) with the Energetic Quantum Limit [5,6] which presents the ultimate limit of the sensitivity for any given energy $\mathcal{E}$:

$$\xi^2_{EQL} = \frac{\mathcal{E}_{SQL}}{2\mathcal{E}}\,. \tag{134}$$

The variation measurement traditional form sensitivity is defined by this formula too. Comparing the values (133) and (134) it is possible to conclude that the "price" for the hardware

setup independance on the signal shape is the pumping energy $720/\pi^4 \approx 7.4$ times higher than for the usual variation measurement, or sensitivity about $\sqrt{720/\pi^4} \approx 2.7$ times lower for the same pumping energy value.

It is worth noting that it can be reasonable to use the harmonic oscillator as a probe system because in this case the given sensitivity can be obtained using the pumping energy approximately 0.7 times less than for a free probe mass.

It should be noted also that for our opinion the more sophisticated expansion of the signal can be constructed, which allows variation measurement with periodical precalculated law for the local oscillator phase time-dependance. The wavelet technology looks especially promising here.

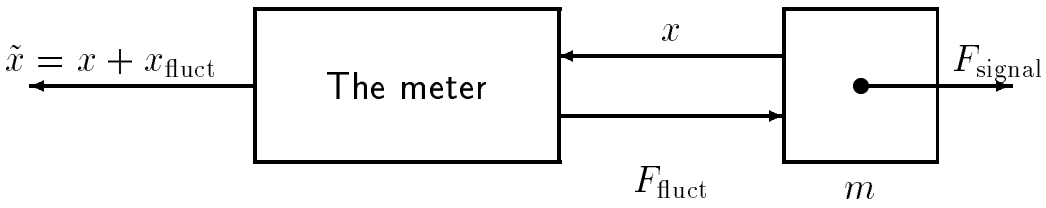

FIG. 6. Abstract scheme of the position meter

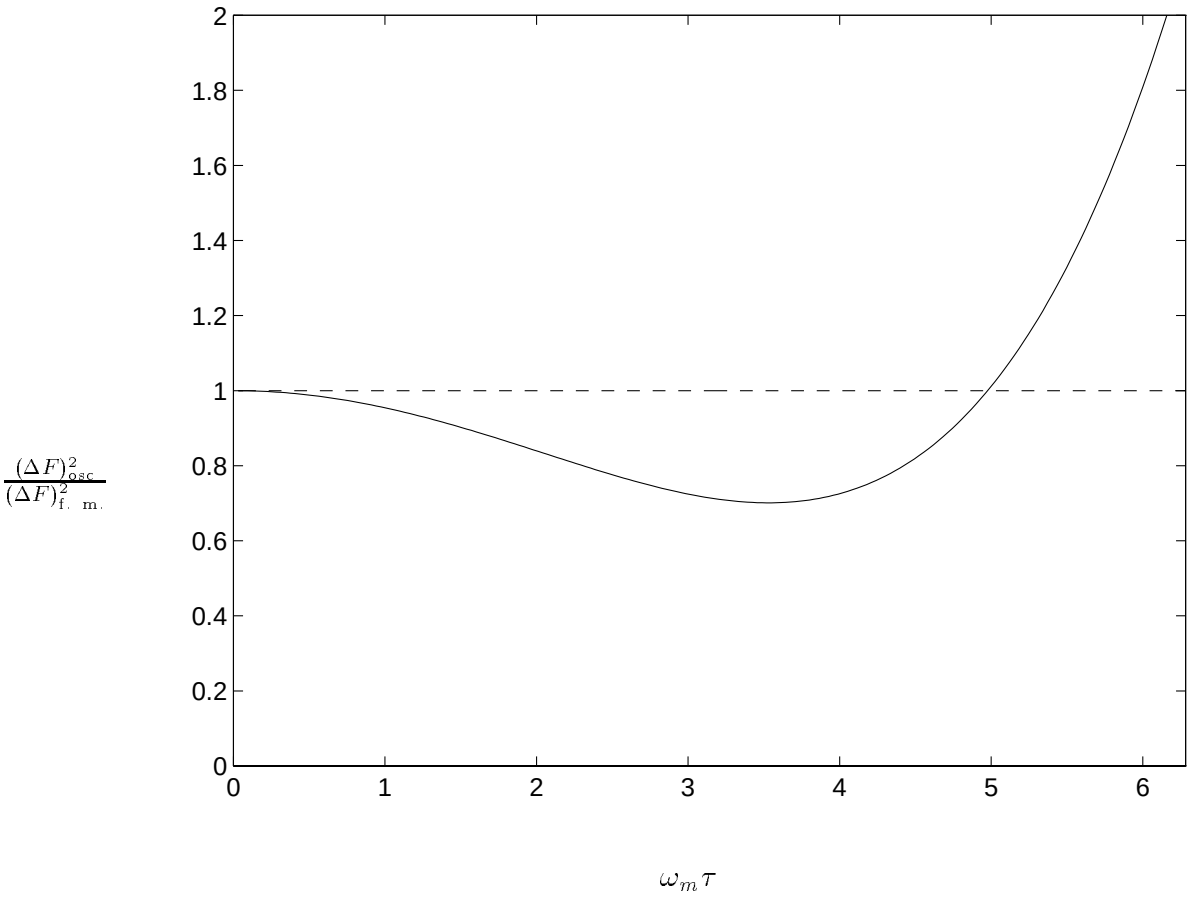

FIG. 7. Measurement errors for the harmonic oscillator relative to the one for the free mass

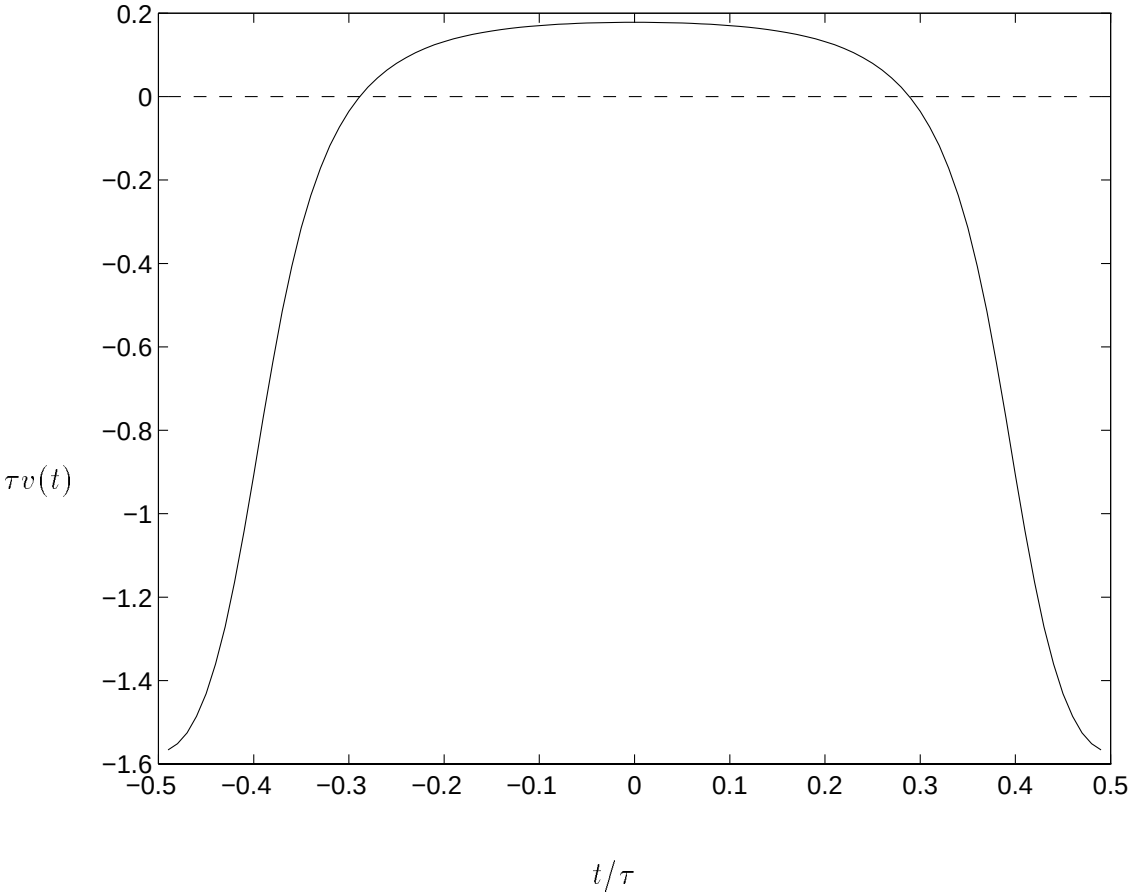

FIG. 8. Optimal filter function for the free test mass

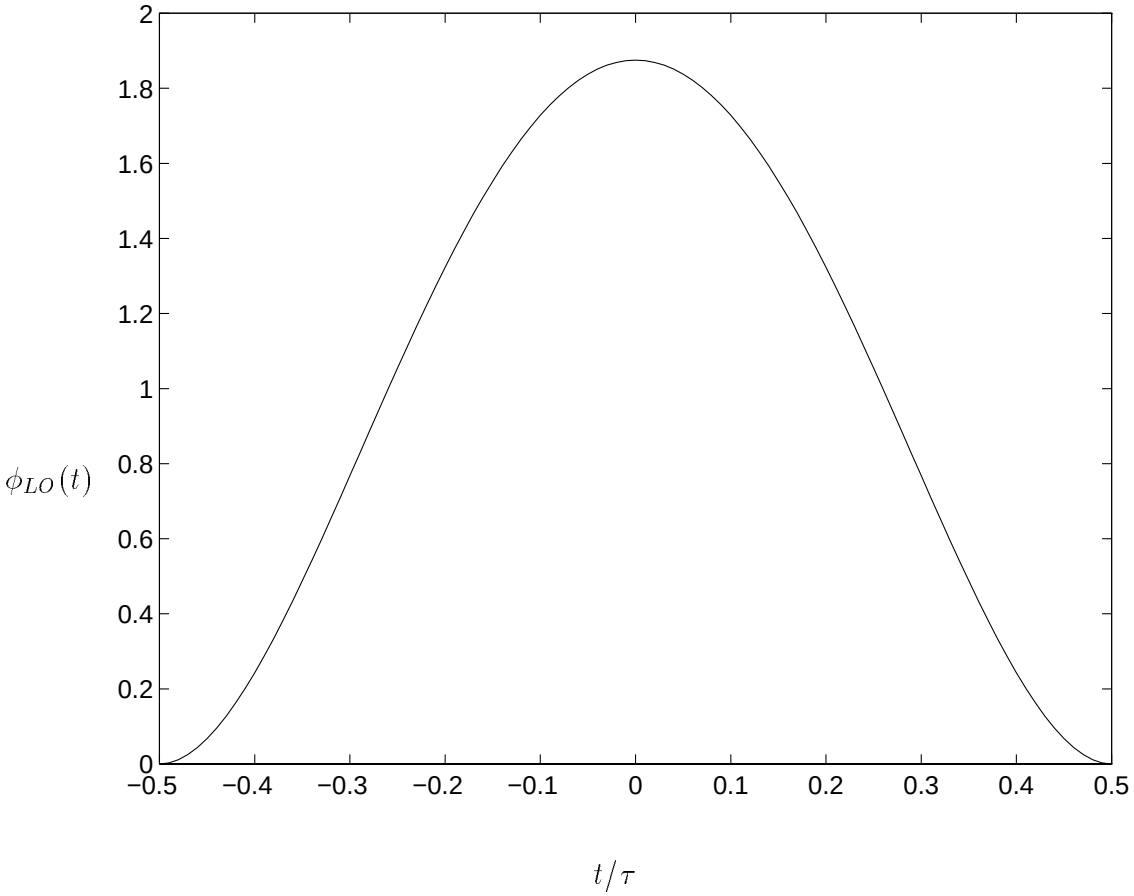

FIG. 9. Phase of local oscillator for the free test mass ($\xi = 1/3$)

REFERENCES

[1] V.B.Braginsky, Yu.I.Vorontsov, K.S.Thorne, Science 209 (1980) 547.

[2] S.P.Vyatchanin, Phys.Lett. **A239** (1998) 201.

[3] S.P.Vyatchanin, E.A.Zubova, Phys.Lett. **A201** (1995) 269.

[4] S.P.Vyatchanin, A.Yu.Lavrenov, Phys.Lett. **A231** (1997) 38.

[5] V.B.Braginsky, F.Ya.Khalili, *"Quantum measurement"*, ed. by K.S.Thorne, Cambridge Univ. Press, 1992.

[6] V.B.Braginsky, M.L.Gorodetsky, F.Ya.Khalili and K.S.Thorne, "Energetic Quantum Limit in Large-Scale Interferomters", proceedings of Third Edoardo Amaldi Conference, Pasadina, 1999.